

Filamentary structure of wind blown superbubbles

Birgitta Müller



München 2011

**Filamentary structure
of wind blown superbubbles**

Bachelor-Assignment

at the

Ludwigs-Maximilians-Universität München

submitted by

Birgitta Müller

(Matr. Nr.: 8066403)

born on 15th of June 1988 in Vilsbiburg

supervised by

Prof. Dr. Andreas Burkert

and

Evangelia Ntormousi

Landshut, 11th of September 2011

Evaluator: Prof. Dr. Andreas Burkert

Directory

| | |
|--|-----------|
| Introduction..... | 1 |
| 1. Theoretical Basis..... | 4 |
| 1.1 Interstellar medium..... | 4 |
| 1.2 Turbulence..... | 6 |
| 1.3 Determining the fractal dimension..... | 7 |
| 1.4 Disturbances..... | 10 |
| 2. Box-counting method..... | 15 |
| 3. Fractal dimension..... | 19 |
| 3.1 Simulations..... | 19 |
| 3.2 Fractal dimension for different thresholds of density..... | 24 |
| 3.3 Comparison to area filled with gas..... | 30 |
| 3.4 Fractal dimension over time..... | 32 |
| Summary..... | 35 |
| Acknowledgement..... | 36 |
| Appendix..... | 38 |
| Bibliography..... | 45 |
| Selbstständigkeitserklärung..... | 47 |

Introduction

There are two possibilities for stars to reduce the amount of hydrogen in their atmospheres: High mass stars produce so-called Ring Nebulae whereas low mass stars produce Planetary Nebulae. What they have in common is that one can see a Wolf-Rayet spectrum below the photosphere caused by dense and fast winds that generate stellar wind bubbles around the stars. This spectrum shows bright emission lines.

Planetary Nebulae show overarching symmetries but in Ring Nebulae one can observe an irregular filamentary forms produced by different velocities of the wind. Those stellar wind bubbles can be parted in two types. On the one hand one has the radiative type which is also called the momentum-driven type and on the other hand obviously the non-radiative type. Which kind of stellar wind can be found depends on the cooling system. The high metallicity found in stellar winds of massive stars often implicates bigger radiative cooling rates but not only that factor but also certain time scales determine whether one has a radiative or non-radiative stellar wind bubble. To be more accurate the type is set by the crossing time for the free wind t_{cross} , the age of the bubble t and the cooling time t_{cool} .

If the cooling time is much smaller than the crossing time ($t_{\text{cool}} \ll t_{\text{cross}}$) for the free wind the bubble is radiative. On the other hand if the age of the bubble is much smaller than the cooling time ($t \ll t_{\text{cool}}$) the bubble is non-radiative. Bubbles can also be partially radiative. That's the case if $t_{\text{cross}} \ll t_{\text{cool}} \ll t$ so that the cooling has an affect on the wind but at the same the time bubble is almost everywhere full of hot shocked gas. If such a shocked wind is found the bubble is energy-driven otherwise it's momentum-driven.

Although a focus will be set on the high mass stars in the following text there now will be a short overview of Planetary Nebulae of low mass stars, too. Those stars are carbon-rich. Observing the atmosphere of the stars one can see that the mass loss rates are about ten times higher in comparison to normal stars although the velocity of the wind there is just like that in

normal central stars. The evolution of the stellar wind especially in the Asymptotic Giant Branch-Phase is not understood yet but according to Dwarkadas and Balick (1998) the evolution of fast wind follows this relation:

$$v_{fw} = v_{fw}(0) \left(1 + \frac{t}{\tau}\right)^\alpha$$

Here the initial velocity $v_{fw}(0)$ is 25 km s^{-1} and $\alpha=1.5$. At last τ is set so that at $t = 3000 \text{ yrs}$ v_{fw} is equal to 2000 km s^{-1} .

For a radiation-driven wind the mass loss changes in a way so that $\dot{M}_{fw} v_{fw}$ is always constant. Although one can say something about the transition velocity no one can make a statement about the transition time as the flow of the wind is not well understood.

More interesting now is the behaviour of Ring Nebulae. Numerical experiments from Garrelt Mellama and Peter Lundqvist (2002) who worked with winds running into a Red Super Giant wind which has the effect that the otherwise complicated description can be handled now like the model for Planetary Nebulae – only with higher mass loss rates – showed that winds from cooler nitrogen-rich stars switch from momentum-driven to energy-driven types. Hotter nitrogen-rich stars as well as carbon-rich stars (both hotter and cooler types) are energy-driven from the start.

In order to say something about the type of wind one can also examine momentum and kinetic energy of the shell and compare it with the energies given by the stellar wind. Here the ratio of shell momentum to wind momentum is π :

$$\pi = \frac{M_{shell} v_{shell}}{\dot{M}_{fw} v_{fw} t}$$

and the ratio of kinetic energies of shell and wind is ϵ :

$$\epsilon = \frac{M_{shell} v_{shell}^2}{\dot{M}_{fw} v_{fw}^2 t}$$

For both ratios the velocities of slow winds are close to zero which may not be correct since often $\dot{M}_{fw} v_{fw} \sim \dot{M}_{sw} v_{sw}$.

An exact ratio for the energy-driven case is not easy to be estimated as the expansion velocity is difficult to describe. However as long as $\dot{M}_{fw} v_{fw}^2 \ll \dot{M}_{sw} v_{sw}^2$ is valid we have

$$\pi_e \approx \frac{1}{3} \frac{v_{fw}}{v_{s,e}} + \frac{1}{3} \frac{v_{fw} v_{sw}}{(v_{s,e})^2}$$

$$\epsilon_e = \frac{1}{3} + \frac{1}{3} \frac{v_{sw}}{v_{s,e}} \left(2 + \frac{v_{sw}}{v_{s,e}} \right)$$

as $v_{s,e} = \left(\frac{1}{3} \frac{\dot{M}_{fw}}{\dot{M}_{sw}} v_{fw}^2 v_{sw} \right)^{1/3}$.

For the momentum-driven types the ratios can exactly be given:

$$\pi_m = \frac{v_{fw}}{v_{fw} + v_{s,m}} + v_{sw} \frac{v_{fw} - v_{s,m} - v_{sw}}{v_{s,m} v_{fw} + v_{s,m}^2}$$

$$\epsilon_m = \frac{v_{fw} v_{s,m}}{(v_{fw} + v_{s,m})^2} + v_{sw} \frac{v_{s,m} (2 v_{fw} - v_{s,m}) + v_{sw} (v_{fw} - 2 v_{s,m} - v_{sw})}{v_{s,m} (v_{fw} + v_{s,m})^2}$$

with $v_{s,m} = \sqrt{\frac{\dot{M}_{fw}}{\dot{M}_{sw}} v_{fw} v_{sw}}$.

A partially radiative character of the stellar wind bubble reduces the values for π and ϵ .

Although Planetary Nebulae show big symmetries the non-linear instability of the thin shell can lead to a fragmented nebula, which can also show a substructure of fragments. In Ring Nebulae the inhomogeneity of stellar winds cause areas of different temperatures and densities. Those parts show a behaviour of dropping temperature and raising density.

1. Theoretical Basis

1.1 Interstellar medium

Gas found in the interstellar medium in the shape of hydrogen can be parted in two types: atomic and molecular gas. Depending on what kind of type is found the appearance is diffuse. The density of hydrogen isn't very high if the gas is atomic. If the gas is molecular, one can observe a rather irregular and fragmental look with dense and cold gas. The Giant Molecular Clouds are the largest objects hold together by self-gravity between different galaxies. Their maximum size amounts to about 100 pc with a maximal mass of $10^6 M_{\text{sun}}$. The question what the smallest size could be is more difficult to answer since there are no clear effects like the galactic shear, that takes action as a too great potential in a galaxy causes tidal forces. Observations however led to the assumption that 10 – 20 AU (astronomical units) might be the minimum of size for molecular clouds. Whether there are smaller shapes or not can't be said yet because the instruments used to investigate the interstellar medium don't have a sufficient resolution and they aren't sensitive enough yet.

Furthermore so-called “extreme scattering events” (ESE) of radio sources – events in which the flux density of e. g. quasars drops by a big amount for multiple weeks or even months – disturb the formation process of molecular clouds. The number of such disruptions is by a factor of 10^3 higher than the number of stars of a near galaxy. Then why are the structures of those molecular clouds so stable and have a comparatively long life time? Walker and Wardle tried to answer this question with the idea of self-gravity. If the clouds then really are gravitationally bound, they would have a mass of about $10^{-3} M_{\text{sun}}$ with an average density around 10^{10} cm^{-3} . These would be the smallest structures theories could foretell. If these suggestions are right then the range of size and masses would be at orders of 6 (for size) and 10 (for masses).

However observations and simulations of Dobbs, Burkert and Pringle (2011) showed that most of the molecular clouds in the interstellar medium aren't all over gravitationally bound. Of course self-gravity is crucial for star formation so how can this statement be right? The answer is that clouds are only gravitationally bound to a certain degree of at most 30% of the volume where the gas is dense enough for star formation.

Motivation for this assumption can be found by considering the virial theorem or more precisely the virial parameter α :

$$\alpha = \frac{5\sigma_v^2 R}{GM}$$

σ_v is the line of sight velocity dispersion and R the radius of the cloud. For $\alpha=1$ which means there is virial equilibrium the virial theorem would be $2T+W=0$ where T is the kinetic and W the potential energy. So the variance of α can say something about the influence of gravity in a molecular cloud and hence something about the cloud being bound or not.

Observations showed that, for most of the clouds, α is different from and bigger than 1. With that unbound and turbulent molecular cloud, where $\alpha > 1$ and even $\alpha > 2$ there would be no star formation all over the cloud's volume but only at some special parts where the density of hydrogen is large enough. Simulations from Bonnell et al. (2010) showed that stellar clusters really formed in bound regions. In addition simulations from Dobbs, Burkert and Pringle (2011) showed that molecular clouds with star formation efficiencies of $\epsilon = 5$ or 10% are nearly everywhere unbound and values for α are in agreement with observations. Clouds with $\epsilon = 1$ per cent are mostly bound and have higher masses which doesn't fit with observations.

1.2 Turbulence

Turbulences in molecular clouds are an important factor for formation processes in the interstellar medium. One quantity to estimate how turbulent the clouds are is the Reynolds number R_e :

$$R_e = \frac{vl}{\nu}$$

with v the velocity, l the characteristic linear dimension and ν the kinematic viscosity. If

$R_e \gg 10^3$ then the medium is said to be turbulent. Typical for turbulence is a fluctuation of density as well as pressure and the presence of many whirls. An estimation for the viscosity can be done if the macroturbulent velocity or the dispersion and the the mean-free-path of cloud-cloud collisions are known. Observations showed that the Reynolds number lies around 10^9 and thus the interstellar medium is highly turbulent.

The so called Larson relations as a sign for the Kolmogorov cascade give a picture where energy causes heat in low scales and is injected in large scales. If the energy transfer rate $v^2/(r/\nu)$ is constant then

$$v \propto r^{1/3}$$

This relation is close to what observations show. As a source of energy at large scales the galactic rotation and shear could be possible. Different factors like the interstellar medium being supersonic and thus dissipative as well as the possibility of energy being provided by stellar formation could lead to the relation

$$v \propto r^{1/2}$$

known as the Burgers spectrum. To what amount magnetic fields are important isn't sure as observations show a equipartition of magnetic and kinetic energy. Because of that the magnetic field is a important factor for energy exchange but on the other side it has no effect on cloud collapse or gravitational instabilities.

Strong fluctuations of density (and also velocity) in the interstellar matter play an important role as the chaos one sees at first sight is no disorder without any chance to look through it but there is a great order within the chaos making it possible to get a self-similar structure over some orders of magnitude in mass and scale. The correlation functions then act like power-laws where the correlation length is infinite.

With the size-linewidth relation $\sigma \propto R^{1/2}$ and the observed scaling law of $\rho \propto R^{-1}$ then one can say:

$$\sigma \propto \rho^{-1/2}$$

and as the turbulent pressure P is defined as

$$\frac{dP}{d\rho} = \sigma^2$$

and with that

$$P \propto \log \rho$$

1.3 Determining the fractal dimension

The main part of molecular gas in the interstellar medium gets its material from expanding and sometimes colliding shells produced by stellar wind and supernovae. Most of it is found in molecular clouds and its structure – as observations have shown and is mentioned above – is very fractal and clumpy. There are also irregular substructures so – if you make an approximation and say that to a certain degree those structures show self-similar behavior in wide ranges (down only to certain scales where specific boundary effects appear) – you can calculate its fractal dimension. The idea of fractals was first introduced by Mandelbrot in 1982 in order to make statements about the homogeneity of systems like molecular clouds and to describe what fraction of space is filled (here with hydrogen). The fractal geometry of such clouds which is due to turbulences and – as some assume – self-gravity affects the evolution of structures in the interstellar medium. The method of how the fractal dimension is calculated will be explained later but for now there will be given an overview of what one can get by knowing the fractal dimension.

As one can only observe the surface of molecular clouds there can only be given a dimension of the fractal structure with a maximum of 2. The relation of the dimension of those cloud-projections to the three-dimensional ones is not known yet but it could be something about $D_{\text{per}} + 1$. D_{per} here is the fractal dimension of the projected cloud calculated by the perimeter-area method. Although this method is not used for getting the fractal dimension of the simulation used for this thesis there will be a explanation of what it is since it can give a good orientation for checking whether the calculated dimension is in an acceptable range. “if the isocontours exhibit a power-law perimeter-area relation with a noninteger exponent over a certain range of scales, this exponent may be interpreted in terms of fractal dimension...”¹ Some people such as Elmegreen and Falgarone (1990) confined values of D_{per} to a range of $1.2 < D_{\text{per}} < 1.5$ and especially $D_{\text{per}} = 1.35$ and so $D_f = D_{\text{per}} + 1 = 2.35$.

The projected dimension of a fractal with actual three-dimensional arrangements has a maximum of 2 so one can say:

$$D_{\text{pro}} = \min \{2, D_f\}$$

as D_f is the three-dimensional fractal dimension of the projected structure. Perimeter P and area A here follow the relation:

$$P \propto A^{D_{\text{pro}}/2}$$

Compared to that there were made simulations and calculations of also the average correlation and mass dimensions of the projections.

For both methods r is the size of cells of a grid laid over the projection.

The correlation dimension is given by

$$D_c = \lim_{r \rightarrow 0} \frac{\log C(r)}{\log r}$$

where $C(r)$ is the correlation integral:

$$C(r) = \frac{2}{N_p(N_p - 1)} \sum_{1 \leq i < j \leq N_p} H(r - |x_i - x_j|)$$

1 Néstor Sánchez, Emilio J. Alfaro, Enrique Pérez: “The fractal dimension of projected clouds”, 2005

N_p is a set of points with position x and in the summation there is count the number of pairs where $|x_i - x_j| < r$ while H is the Heaviside step function.

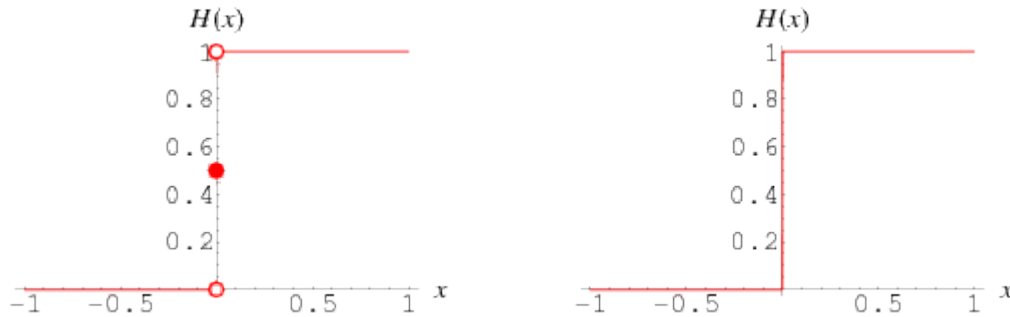


Figure 1: from <http://mathworld.wolfram.com/HeavisideStepFunction.html>; Heaviside step function

The mass dimension follows a more simple law:

$$M(r) \sim r^{D_M}$$

A focus will be set on this kind of dimension later on as the parameters given from the simulations that were used for this assignment show the density distribution of hydrogen in the wind-blown superbubbles.

Using these methods the results for the values of D_f are now $D_f \approx 2.6 \pm 0.1$. So by knowing the fractal dimension one can make statements about the distribution functions of size and mass of the clouds and moreover, about the initial mass function of the centered star.

1.4 Disturbances

Theoretically determining the fractal dimension by using the perimeter-area dimension method and the mass-size dimension method is an acknowledged method. Different factors however influence the values one gets for the fractal dimension. Those factors are opacity and noise observed in the interstellar medium.

While opacity has no influence on the output of D_{per} there will be a different result for the mass dimension D_m as it gets bigger as opacity grows. In addition the estimation of D_{per} is influenced by the resolution of the observed fractal as well as by the emission of the cloud as particles closer to an observer hide from the back side of the cloud. However since we use simulations those problems won't be handled in the following text.

Opacity

Simulations of earlier fractals in the interstellar medium were done under the approximation of an optically thin cloud as there was made the assumption that every particle behaves like another one. What happens to the estimation of the fractal dimension if this approximation isn't set anymore will be shown now. Contributions are weighted by $\exp[-\tau(x,y)]$ for the plane $z=z_0$ where

$$\tau(x,y) = c \int_{z_0}^z \rho(x,y,z) dz$$

is the total optical depth between the point (x,y,z) and the projection plane. In the absorption constant c there are some parameters like the mean molecular weight or the abundance of the emitting molecule contained. The maximum optical depth τ_0 for the case that the complete mass M_f is homogeneously distributed in the outright usable volume

$$V_f = \frac{4}{3} \pi R_f^3$$

is for $M_f=1$ and $R_f=1$:

$$\tau_0 = \frac{3c}{(2\pi)}$$

The total optical depth then is close to τ_0 because it is a function of the position in the observed area. So for example $\tau \approx 0.9$ for $\tau_0 = 1.0$ and $\tau \approx 1.7$ for $\tau_0 = 2.0$. How does this influence the assessment of D_f ? In order to say something about that we now look again at the parameter-area based dimension and the mass dimension.

Using the method of determining D_{per} mentioned above calculations have shown that D_{per} isn't affected by the opacity and that discrepancies always lie in line with expected degrees. The following figure shows that for different threshold intensities – where the intensity of pixels are above this threshold – the fractal dimension (represented by the fitting line's slope) is always nearly the same.

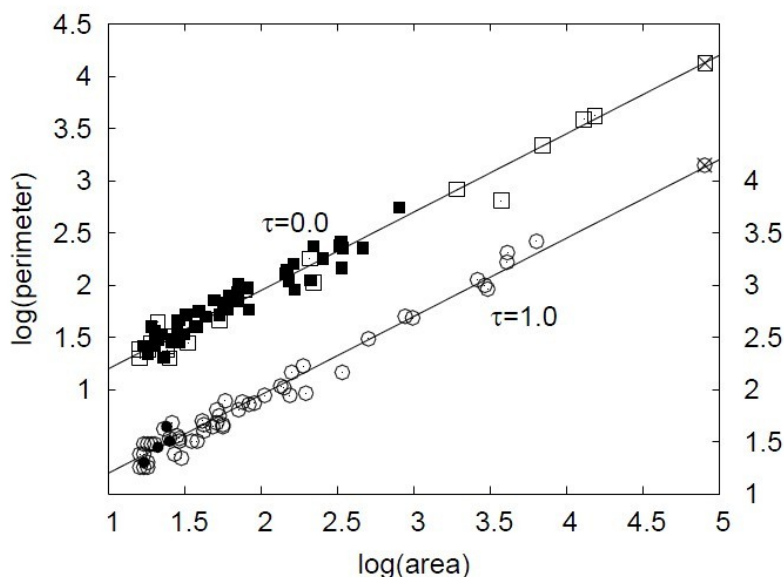


Figure 2: from Sánchez et al. (2005); perimeter plotted against the area in both logarithmic ways; the slope (and with that the fractal dimension) is nearly the same for both total optical depths. The intensity levels are fixed at 25% (crossed symbols), 50% (open symbols) and 75% (filled symbols) of the maximum intensity.

For higher thresholds one can examine smaller and denser structures, but very dense parts can hardly be detected because opacity covers the structure near such cores. Nevertheless, as we have only one fractal examined the properties of this fractal are the same and so the fractal dimension and with it the perimeter-area based dimension is not affected by the opacity.

That is different for the mass dimension method. As to say something about the mass dimension, one needs to know how the particles are distributed at every point of the cloud (cf. $M(r)$). Without this parameter it will not be possible to give a good estimation of D_m . So the inner and dense regions – which could as mentioned above be occulted by the outer regions and projections – are important for determining $M(r)$. Observations have shown that D_m increases as τ_0 grows. Bigger τ_0 bring about shorter dynamical ranges of intensities and the estimation of D_m becomes already worse at a value of $\tau_0 \geq 1.3$.

Noise

Depending on how strong the emission lines of a fractal bubble are there are low or high signal to noise ratios S/N. Following Vogelaar und Wakker (1994) there has been evidence that contours of fractal stellar clouds – especially for smooth clouds – are distorted by noise and because of that the value one gets for D_{per} increases as there is more noise producing irregular structures. In order to have an overview on how D_{per} and also D_m are affected by the noise there can be used σ as the size of the neighborhood region so as to smooth areal irregularities so that one can say how D_{per} and D_m depend on the noise in a molecular cloud. Calculations and simulations showed that for growing regions σ D_{per} decreases and D_m rises as long as the sound to noise ratio S/N isn't too big.

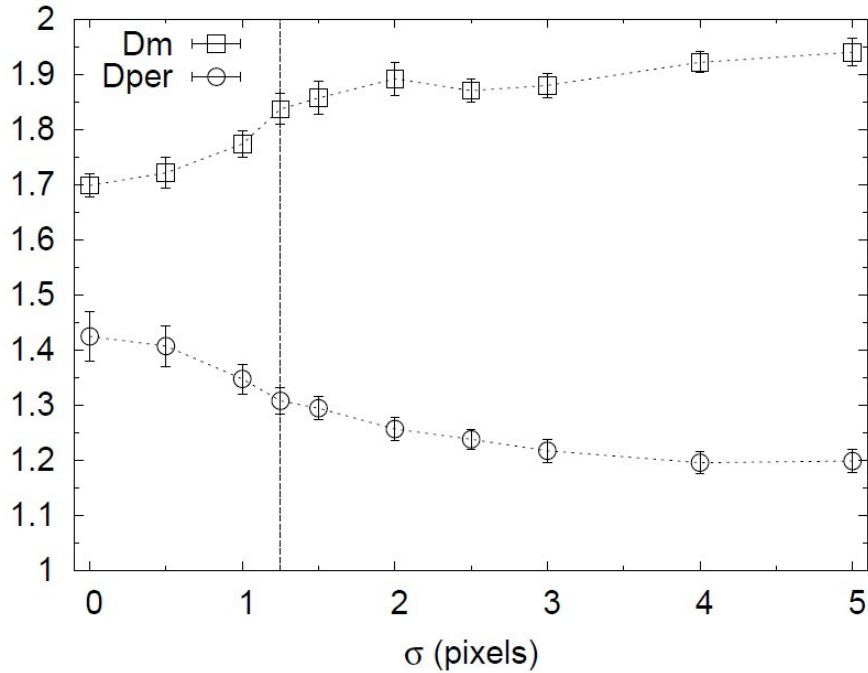


Figure 3: from Sánchez et al. (2005); mass dimension (D_m) and perimeter dimension (D_{per}) in dependence of the smoothing parameter σ ; the dashed line shows the point where the contrast has its maximum.

Again, in order to calculate D_{per} there a certain number of intensity levels can be used. Although the lower ones are disturbed by noise for a high S/N ratio there will be nearly no effect on determining D_{per} as all levels are examined and so in the final result the noise only contributes to a small share. That's different for fractals with a low sound to noise ratio as there the intensity levels and the noise levels don't differ very much. Also the fringe of the molecular clouds could be elongated and thus the result for the perimeter dimension might be higher than expected. One way to solve this problem is to smooth the maps of fractals and flatten the noise of pixels that lie next to each other. The danger in using this method is that one could overdo this smoothing process and so the value for D_{per} becomes too low.

In addition determining the mass is very difficult because hydrogen molecules don't radiate as long as they are cold and furthermore, they are symmetric and have no dipole moment. A possible tracer would be the molecule CO, but the exact ratio to the number of hydrogen molecules (something around 10^{-4}) isn't known yet. Moreover, it is either photo-dissociated or optically thick. Nevertheless, there is a possibility to get a relation between this parameter and the radius of the molecular cloud. Using the size-linewidth relation – or equivalent to the line-width the velocity dispersion σ following power-law can be used

$$\sigma \propto R^q$$

with $0.3 < q < 0.5$.

Assuming the molecular clouds are virialised then one can say:

$$\sigma^2 \propto M/R$$

and thus

$$M \propto R^D$$

where D is the Hausdorff fractal dimension in a range of 1.6 to 2.

2. Box-counting method

There are different possibilities for calculating the Hausdorff dimension. One way is the so called box-counting method. In order to give a motivation for calculating this parameter there will be a definition of what self-similarity is as self-similarity is one crucial attribute of fractal objects such as regions where two wind-blown superbubbles collide as those happenings contribute to a important share to the formation process of the fractal molecular clouds. For explaining the self-similarity the so called Koch curve will be used as an illustrative example. In order to generate a Koch curve one starts with a one dimensional line. This line will be divided into three equal parts and the middle part will be removed and replaced by two sides of a triangle with the same length as the removed part. Now this process will be repeated for the four sides one got in the first step and following this procedure for the next 16 sides and so on.

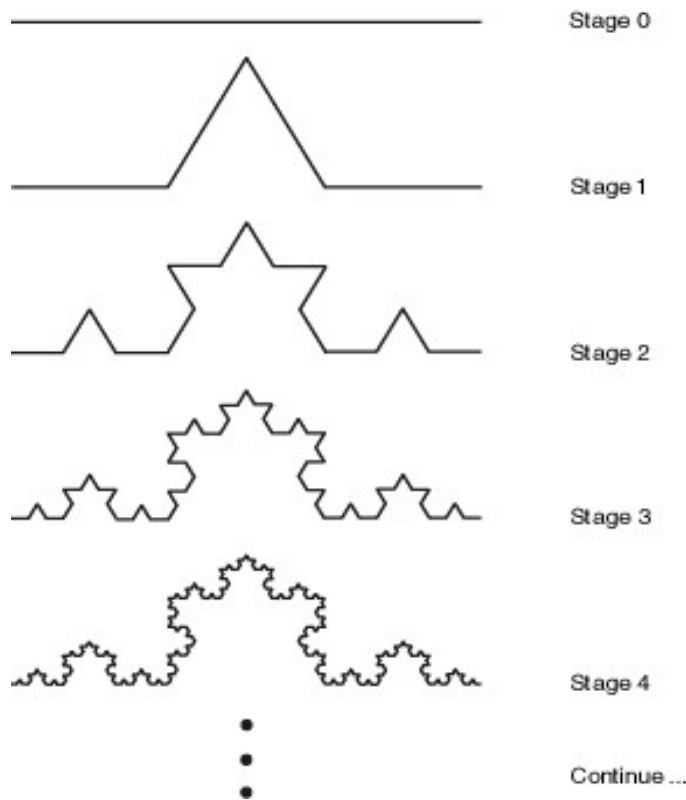


Figure 4: from http://www.nd.edu/~jcaine1/mathematics/limits_chaos.html; generating the Koch curve

Doing this infinitely often one gets the Koch curve:

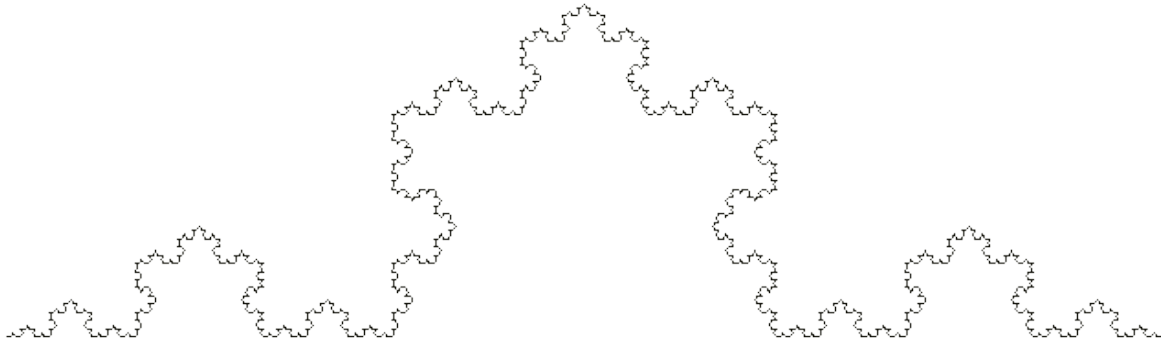


Figure 5: from <http://www.jimloy.com/fractals/koch.htm>; Koch curve

Now self-similarity means that for different scales the examined part of this curve looks just like one another so as you zoom in the structure you will always see the same shape. In order to say something about its fractal dimension the concept of dimension will be explained itself. Examining for example lines, squares and cubes, which are all self-similar objects there can be given a quite good explanation.

By parting a line in e. g. 8 pieces of same length one has to magnify one of these parts by the factor of 8 in order to get the initial line. Same goes for 10 parts where one segments length has to be multiplied by 10 to get the initial line. For 100 or for N parts the magnification factor would be 100 or N . A square in contrast which is parted in 4 equal squares has a magnification factor of 2 since the sides spanning the square have to be doubled in length in order to achieve the initial square. If the square was decomposed in 49 equivalent squares, the magnification factor would be 7 and for N^2 parts it would be N . Same procedure will lead to a relation of N^3 sub-cubes for a magnification factor of N if a cube is examined. Thus the dimension is the exponent of the number of self-similar pieces associated with the magnification factor N . So the (Hausdorff) dimension can be calculated in the following way:

$$D = \frac{\log(\text{number of self-similar pieces})}{\log(\text{magnification factor})}$$

For e.g. a square this would be:

$$D = \frac{\log(N^2)}{\log(N)} = \frac{2 \log(N)}{\log(N)} = 2$$

Examining the process of how the Koch curve is made its dimension will be different from 1 the line has in stage 0 but it won't be 2 either as there isn't generated a plane object. One way to calculate its (fractal) dimension is the so called box-counting method. Using that the Koch curve will be covered by squares whose side length will get smaller and smaller (decreased by always the same factor) and then the number of boxes with self-similar structures will be counted. The box-counting dimension can only be calculated if there is a constant $c > 0$ so that

$$\lim_{L \rightarrow 0} \frac{N(L)}{1/L^D} = c$$

where L is the box' side length and $1/L$ is the magnification factor. With that D is (cf. Definition of dimension written above)

$$D = \lim_{L \rightarrow 0} \frac{\log N(L)}{\log(1/L)}$$

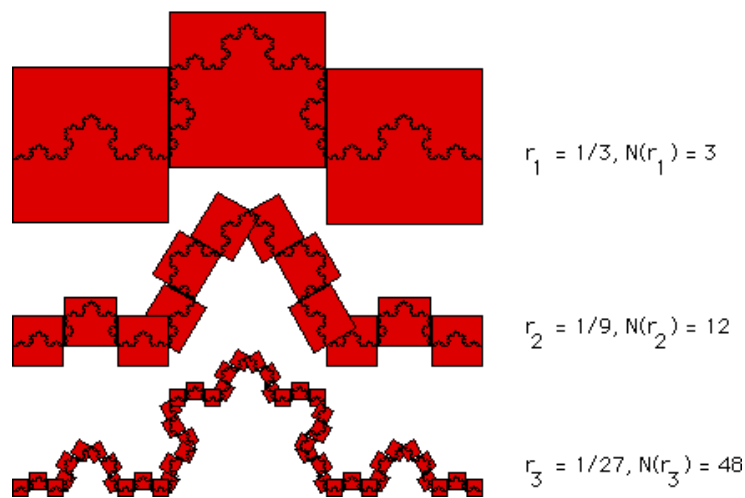


Figure 6: from <http://classes.yale.edu/fractals/fracanddim/boxdim/KochBoxDim/KochBoxDim.html>; Koch curve covered by smaller and smaller boxes

For the example of the Koch curve it is

| Length of box L (Length of initial line =1) | Number of boxes N |
|---|---------------------|
| 1 | 1 |
| 1/3 | 3 |
| 1/9 | 4·3 |
| 1/27 | 4 ² ·3 |
| 1/81 | 4 ³ ·3 |
| (1/3) ⁿ | 4 ⁿ⁻¹ ·3 |

Hence the fractal dimension can be calculated in following way:

$$D = \lim_{L \rightarrow 0} \frac{\log N(L)}{\log(1/L)} = \lim_{n \rightarrow \infty} \frac{\log N(L)}{\log(1/L)} = \lim_{n \rightarrow \infty} \frac{\log(4^{n-1} \cdot 3)}{\log 3^n} = \dots = \frac{\log 4}{\log 3} \approx 1.26$$

In reality there are some factors such as a limited resolution – thus the boxes size can't get infinitely small – and the fact that structures aren't perfectly self-similar cause that the formula above can't be used in a satisfying way. Nevertheless, there is a way to get the fractal dimension of structures like the fractal molecular clouds: By plotting the logarithm of the magnification factor against the logarithm of the number of boxes with structures the slope of a fitting line between the different data points indicates the fractal dimension of the observed object.

3. Fractal dimension

3.1 Simulations

Based on simulations from Ntormousi, Burkert, Fierlinger and Heitsch (2010) who have simulated the hydrodynamical collision of two windblown superbubbles in an uniform as well as in a turbulent diffuse medium the fractal dimension for a section of the meeting area of the colliding region (turbulent case) will be observed. For the simulation there were set some constraints due to computational limits (cf. Ntormousi, Burkert, Fierlinger and Heitsch,2010):

1. The stars belonging to the investigated arrangement all arose at the same time. Time metering starts at the point were stars format in wind areas.
2. The two superbubbles start to expand simultaneously.
3. Metallicity is solar.
4. There is no external gravity field and no self-gravity of the gas.
5. The spacial distributions of stars are regarded as one uniform source with are region radius of 10 pc.
6. There are initial turbulences by the use of a turbulent velocity field.
7. The rout mean square (rms) Mach number is ≈ 1 so the turbulent kinetic energy is equal to the thermal energy of the gas.
8. The driving of turbulences are neglected as the turbulence crossing time in the diffuse medium is with 86 Myr much longer than the calculations time so there are almost no energy losses.

The centres of the expanding superbubbles are 500 pc apart and the simulation time will go up to 7.1 Myr.

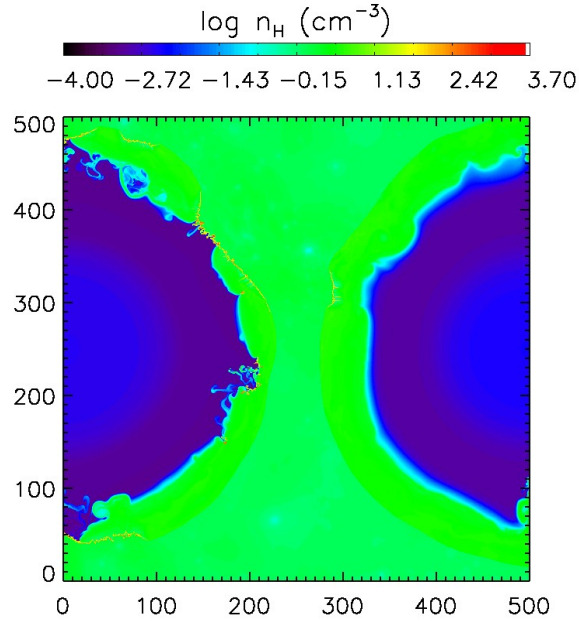


Figure 7: from Ntormousi et al. (2010);
superbubble collision-snapshot for $t = 3.0$ Myr;
the axis' unit is pc

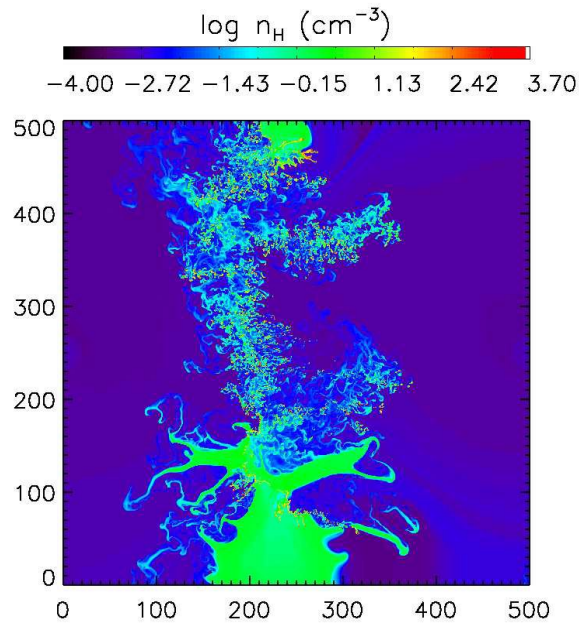


Figure 8: from Ntormousi et al. (2010);
superbubble collision-snapshot for $t = 7.0$ Myr;
the axis' unit is pc

The observed part of the simulation will be the middle box shown in the following Figure:

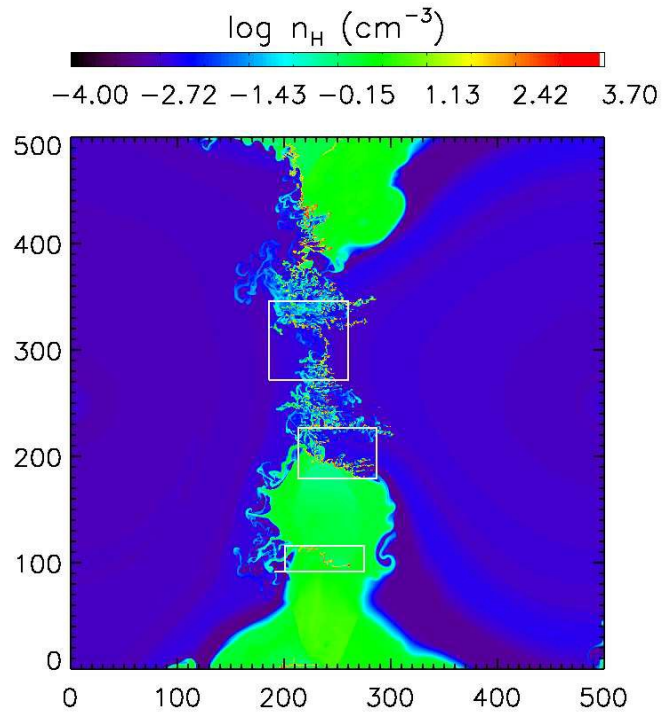


Figure 9: from *Ntormousi et al. (2010)*; snapshot for $t = 5.3 \text{ Myr}$; the plot shows the hydrogen density; the axis' unit is *pc*

Out of the time steps for 4.3, 4.6, 4.8, 5.2, 5.4, 5.7, 6.0, 6.4 and 7.1 Myr where snap shots were made, there will be a arbitrarily set focus one the simulation at the time steps of $t = 4.8$, 5.2 and 6.4 Myr.

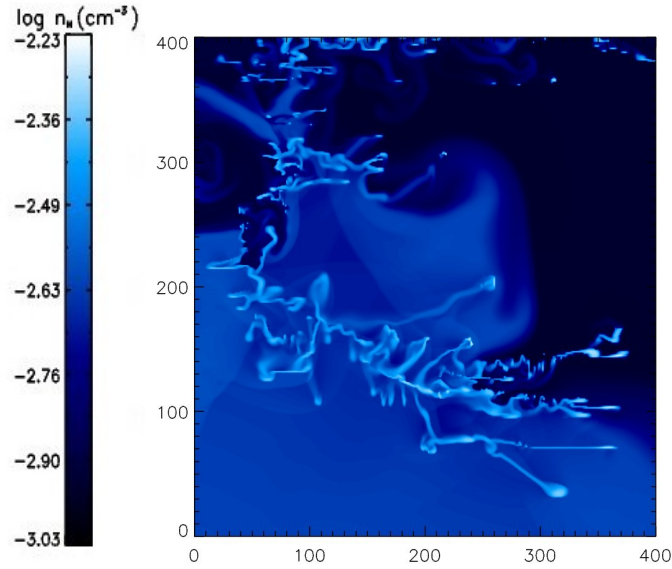


Figure 10: zoom-in snapshot of superbubble collision for $t = 4.8$ Myr; shown is the hydrogen density; the axis unit is the number of datapoints used

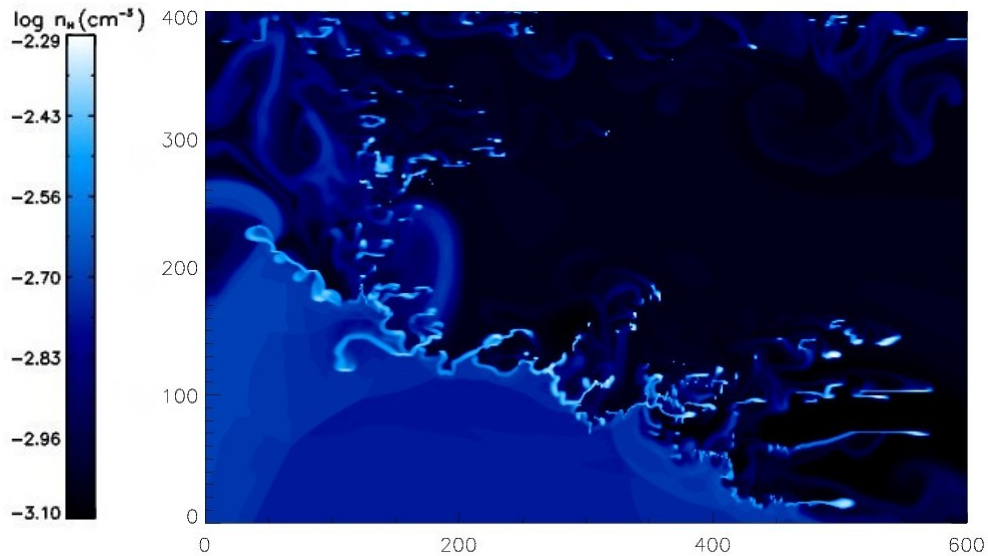


Figure 11: zoom-in snapshot of superbubble collision for $t = 5.2$ Myr; shown is the hydrogen density; the axis unit is the number of datapoints used

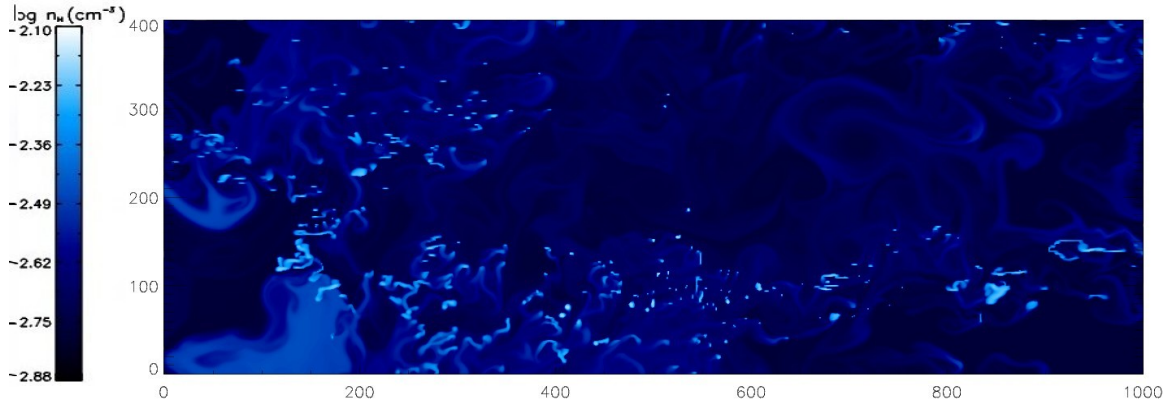


Figure 12: zoom-in snapshot of superbubble collision for $t = 6.4$ Myr; shown is the hydrogen density; the axis unit is the number of datapoints used

Analyzing the development of the cooling gas' density in the box the following statements can be made: The observed gas contained in the first box at $t = 4.3$ Myr expands as time goes on and the matter will agglomerate so the gas will have more and more clumps. The fragmentation process occurs due to different instabilities:

Nonlinear thin shell instability (NTSI): According to Vishniac (1994) dense shells that cool due to radiative processes aren't influenced by linear perturbation but are very instable to the non-linear ones. If the movement of the shell is larger than the thickness of the disk momentum is taken away from the shock of two colliding flows and moved towards trailing regions of the shock. Thus the shell will expand in an unstable way.

Kelvin-Helmholtz instability: Stratified flows show a instable shear layer after a flow separation if the flow hits a blunt object or if two different immiscible liquids or gases with different velocities have contact with each other. Its spatial and temporal expansion is described by the Kelvin-Helmholtz instability.

Thermal instability: On timescales shorter than the dynamical timescale of a cloud it is possible to have cooling instabilities that can bring forth a pressure gradient what in turn causes a gas flow from areas with low density to such with high density. As a result of that density perturbations increase by a big amount.

3.2 Fractal dimension for different thresholds of density

As not only the chronological development is interesting there will be analyzed the fractal dimension for different thresholds of density starting with the simulation snapshot for $t = 5.2$ Myr. Haphazardly chosen thresholds are $\log(n_H(\text{cm}^{-3}))=0.5$ and 2.0.

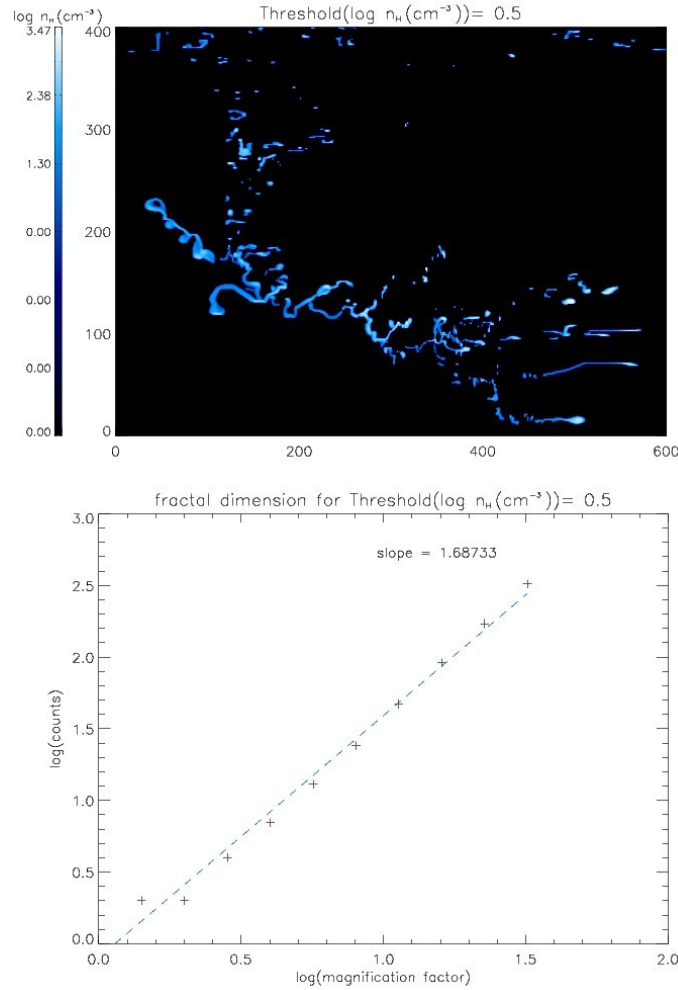


Figure 13: density plot for threshold $\log n_H(\text{cm}^{-3})=0.5$ at $t = 5.2$ Myr (up); below: box-counting plot with the value of D (slope)

The upper image shows the gas' structure where the density is higher than the set threshold (black areas are those where the density is below the threshold) and the lower plot shows the calculated fractal dimension (slope of the line of best fit) by using the box-counting method.

Note that the particle density says something about how many particles there are in a box so that the number of boxes with (self-similar) structures can be counted.

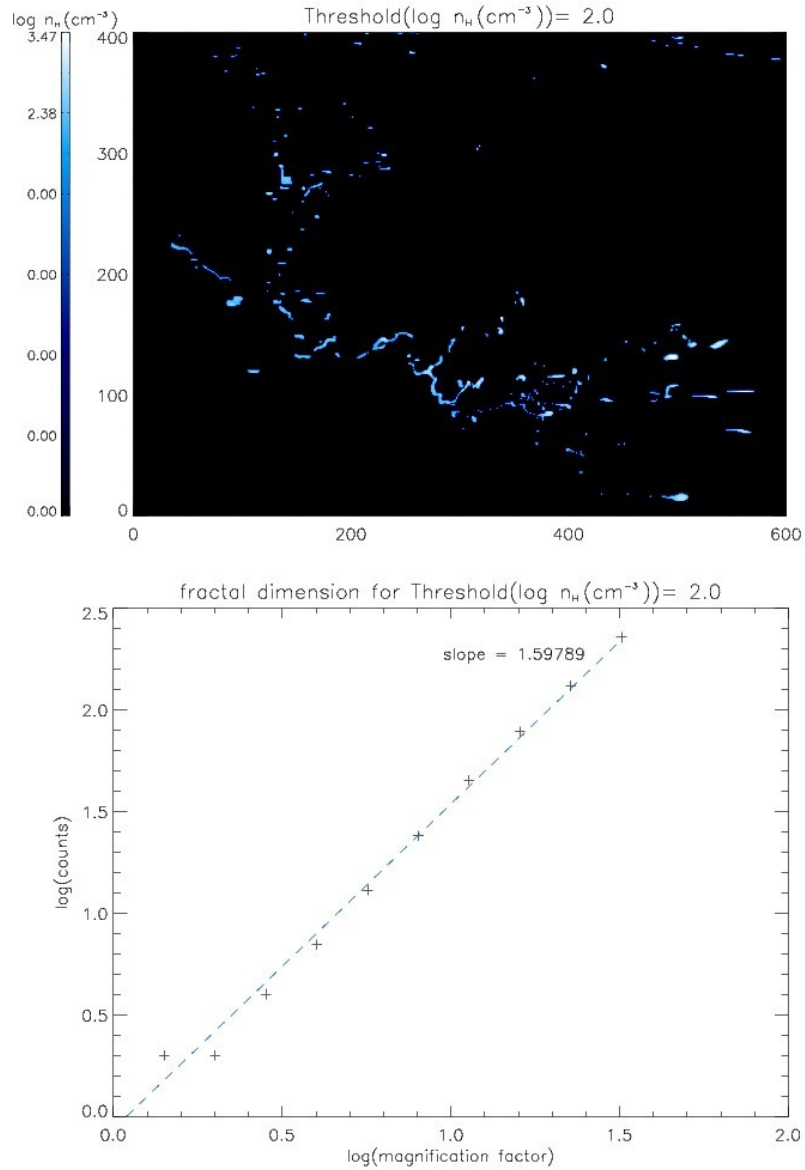


Figure 14: density plot for threshold $\log n_H(\text{cm}^{-3}) = 2.0$ at $t = 5.2 \text{ Myr}$ (up); below: box-counting plot with the value of D (slope)

As the two plots are compared (and also the plots for the other thresholds) there can be seen especially one trend: As the threshold for the hydrogen density of the molecular gas rises, the calculated fractal dimension decreases. This development is apparently correct as for a greater threshold there is more and more structure containing gas taken away from the initial two-dimensional area where every point was considered to be filled with gas. As a result the fractal dimension decreases from a value of to 2 down to a value near (but bigger than) 1. Now what is interesting is the way of how the value decreases:

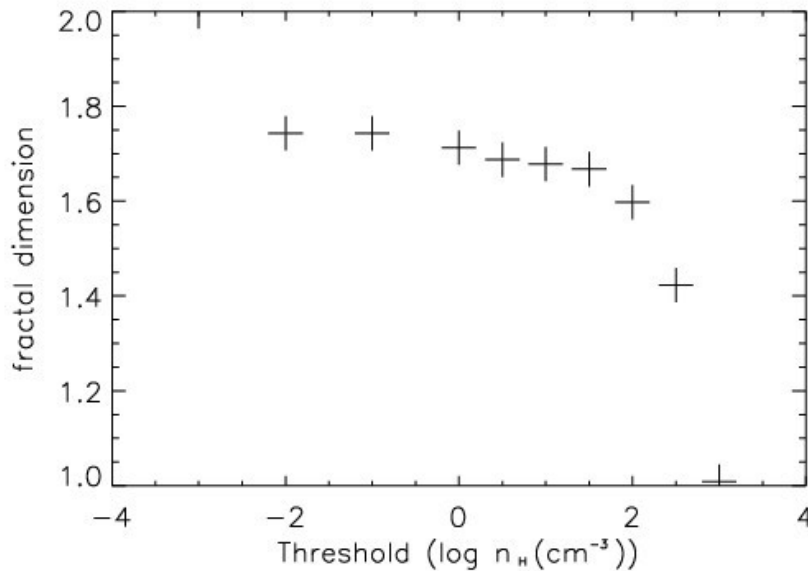


Figure 15: the fractal dimension plotted against the density threshold for $t = 5.2 \text{ Myr}$

Examining this plot there could be made following assumption if there was a superimposed curve that would give a good estimation for the behaviour of the plot's points:

$$D_f \propto -e^{c \cdot \text{th}}$$

where c is a constant that may be calculated in future assignments and th is the hydrogen threshold.

Comparison with e. g. the simulation snapshot for $t = 6.4$ Myr as well as with other time steps shows that this behaviour is similar for each case. Threshold plots are here shown for $\log(n_H(\text{cm}^{-3}))=1.0$ and 2.0.

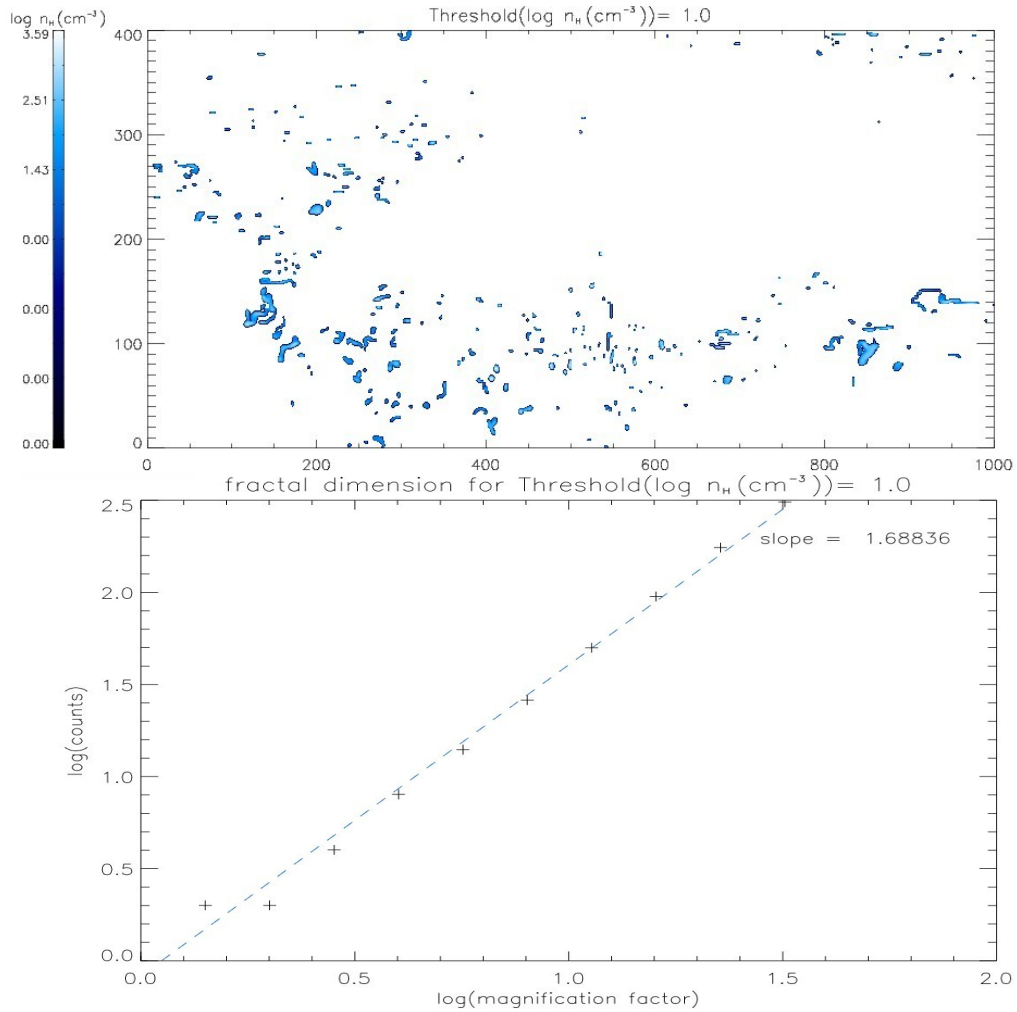


Figure 16: density plot for threshold $\log n_H(\text{cm}^{-3})=1.0$ at $t = 6.4$ Myr (up); below: box-counting plot with the value of $D(\text{slope})$

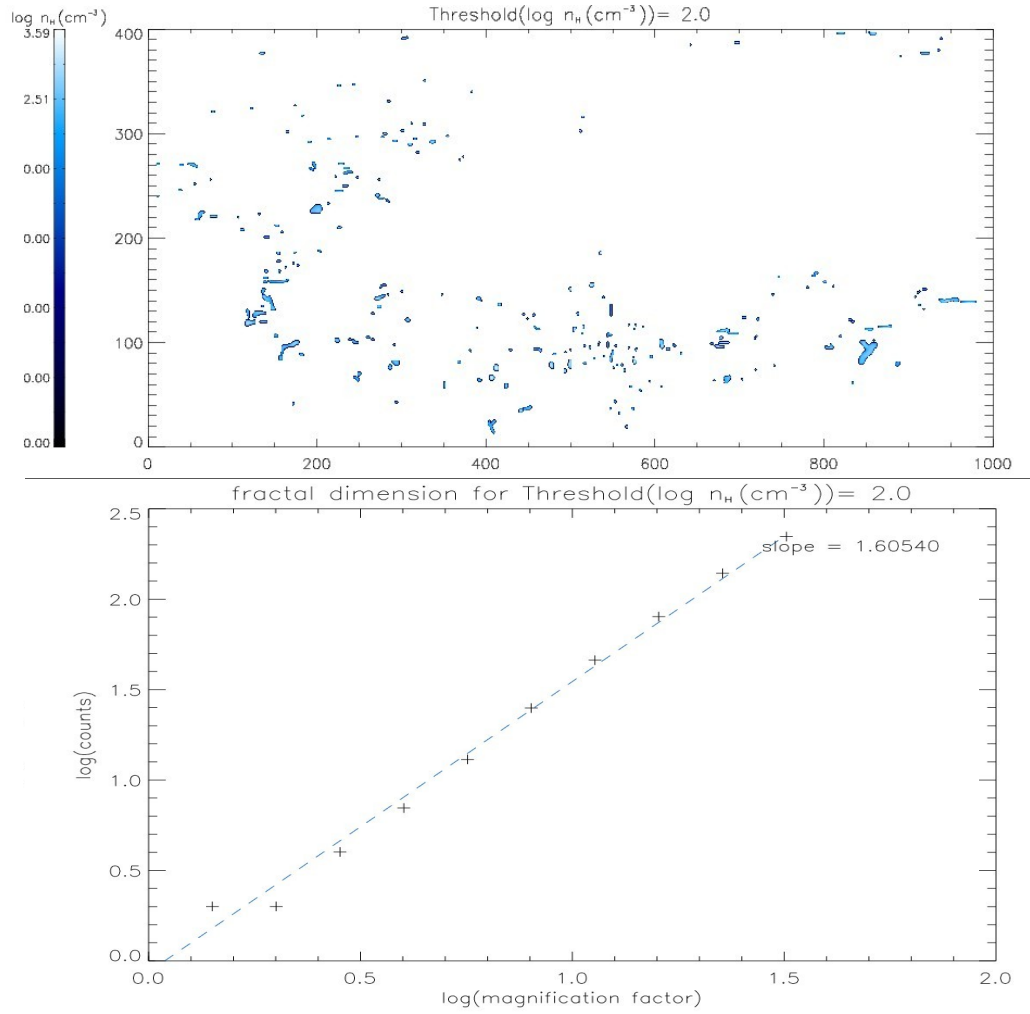


Figure 17: density plot for threshold $\log n_H(\text{cm}^{-3}) = 2.0$ at $t = 6.4 \text{ Myr}$ (up); below: box-counting plot with the value of $D(\text{slope})$

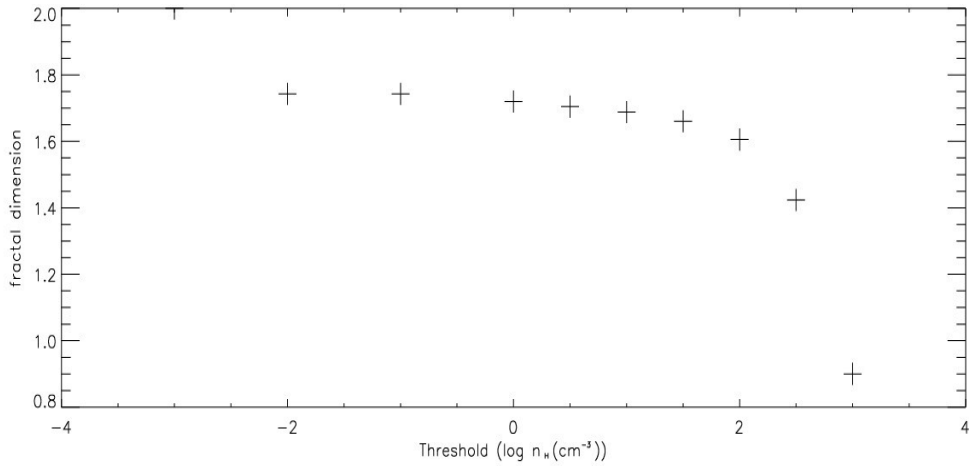


Figure 18: the fractal dimension plotted against the density threshold for $t = 6.4 \text{ Myr}$

One interesting question now would be if this behaviour is valid for simulated fractals in the interstellar medium matches with the behaviour of molecular clouds being observed. Future research could give an answer to that interesting question and with showing to what extend the simulations are in agreement with the observed data there can also be done even better estimations of how close the assumption for the simulations are in comparison to reality.

For the sake of completeness there can be found plots of the simulations with different thresholds of density for each time step in the appendix. In addition, there was also a figure added, where the fractal dimension is plotted against the threshold.

Attention should be payed to the fractal dimension for big thresholds. At some plots there a fractal dimension < 1 can be found although the fractal dimension is supposed to be near but greater than 1. That's because, despite there are more and more clumped regions considered there will never be attained a structure that resembles something similar to a one-dimensional line. So why are there values for $D < 1$? The reason for that can be found in the narrowness of the resolution. The boxes size can't get infinitesimally small and so a correct analysis of the number of boxes where gas can be found isn't possible.

3.3 Comparison to area filled with gas

As the fractal dimension can be a estimation for the complexity of a (almost) self-similar structure and as it can say something about how filled an observed area is it is also interesting to investigate the ratio of the area where gas can be found to the total area examined in dependence of the threshold of hydrogen density. Note that the plots for the area-orientated analysis start for $\log(n_{\text{H}}(\text{cm}^{-3}))=0.0$ as the fractal character starts to get interesting only at this point though there are areas of density with $\log(n_{\text{H}}(\text{cm}^{-3}))$ down to -3.0.

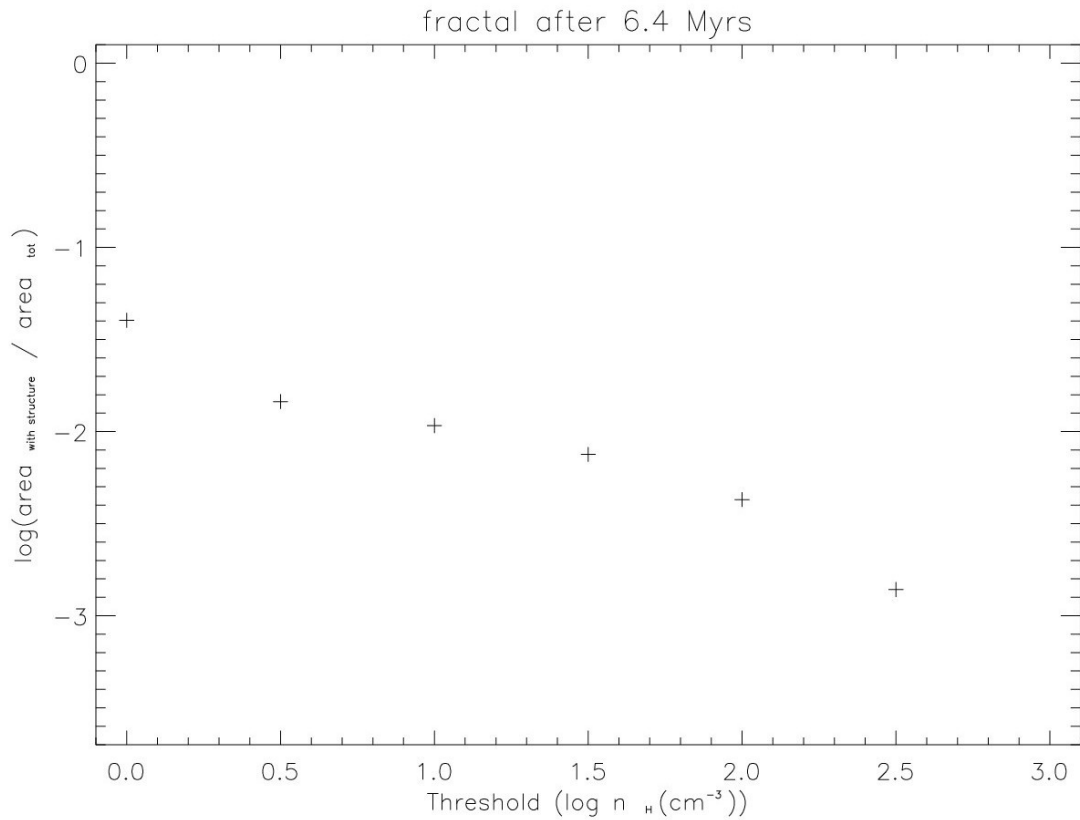


Figure 19: ratio of area filled with gas to total area in dependence of the density threshold

Using the example of the snapshot for $t = 6.4$ Myr (cf. Figure 12) one may notice, that the fractal dimension doesn't change by a big amount, although, there are big changes in the ratio of area with structure to the total area – don't forget here that the y-axis is logarithmic, too, so the apparent resemblance of the two plots doesn't give a clear relation between area a fractal dimension. In those two examples the value for the fractal dimension lies always around 1.8 for $t = 4.8$ Myr or respectively 1.7 for $t = 6.4$ Myr (for thresholds between about 0.0 and 2.0) where the ratio of area with structure to the total area changes by a factor of ≈ 10 . To confirm if this is true for filaments observed in the universe or not might be a task for subsequent research.

As a consequence the fractal dimension is a utile quantity that examines the filamentary structure even if the density varies a lot and even hence if it is difficult to exactly describe the density distribution of the area where the two superbubbles collided.

3.4 Fractal dimension over time

As there has been an analysis for the fractal dimension at a set time segment, but with variable thresholds of hydrogen density there will now be examined how the fractal dimension develops with proceeding time but constant threshold of density. Therefore, there will be shown figures for $\log(n_H(\text{cm}^{-3})) = 0.5$ and 2.0 where the fractal dimension is plotted against the time that has gone by.

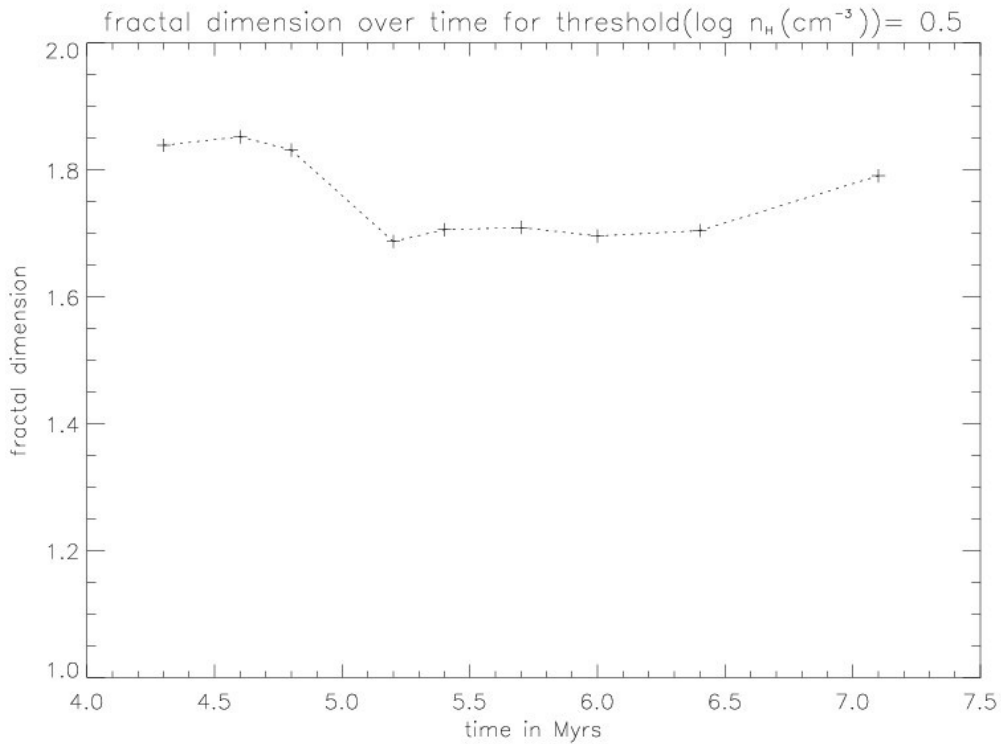


Figure 20: fractal dimension as time goes on; logarithmic density threshold = 0.5

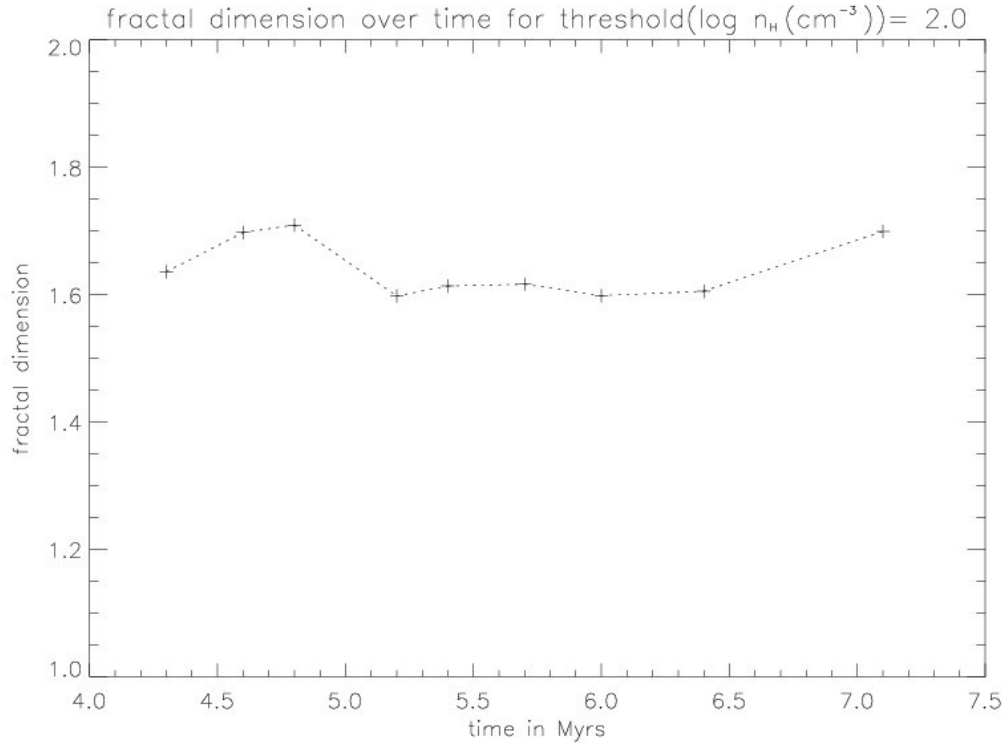


Figure 21: fractal dimension as time goes on; logarithmic density threshold = 2.0

In the plots one can see that the fractal dimension tends to increase for the first time steps – starting from $t = 4.3$ Myr up to 4.8 Myr. An explanation for this behaviour is that in the early phase after the collision of the two superbubbles the hydrogen gas only moves on and that the clumping process hasn't fully started. So there is no fractal appearance that can be comprised by the calculation of the fractal dimension of the gas. After this first time interval – for the time interval from approximately 4.8 Myr to 6.4 Myr – the curve sinks, revealing the fractal shape of the filamentary gas. Here, the value of the fractal dimension decreases as the hydrogen clumps together building the fragmental structure observed. The smaller values of D show that the collision zone of the two superbubbles shows a more and more fractal look. Finally (as of 6.4 Myr) the fractal dimension increases again for late times. The reason

therefore is that the gas that didn't clump disperses making the total picture more plane even at different thresholds.

In conclusion, there will be a shown a plot where all the curves of fractal dimensions in dependence of the elapsed time for the different thresholds in one figure. Here one can see that the behaviour of the curves described above is valid for all thresholds. The discrepancy for the threshold $\log(n_{\text{H}}(\text{cm}^{-3})) = 3.0$ is due to the problem of the limited resolution that was already mentioned. In the plot you can also see the behaviour of decreasing values for the fractal dimension as the density threshold rises that has been shown in 3.2.

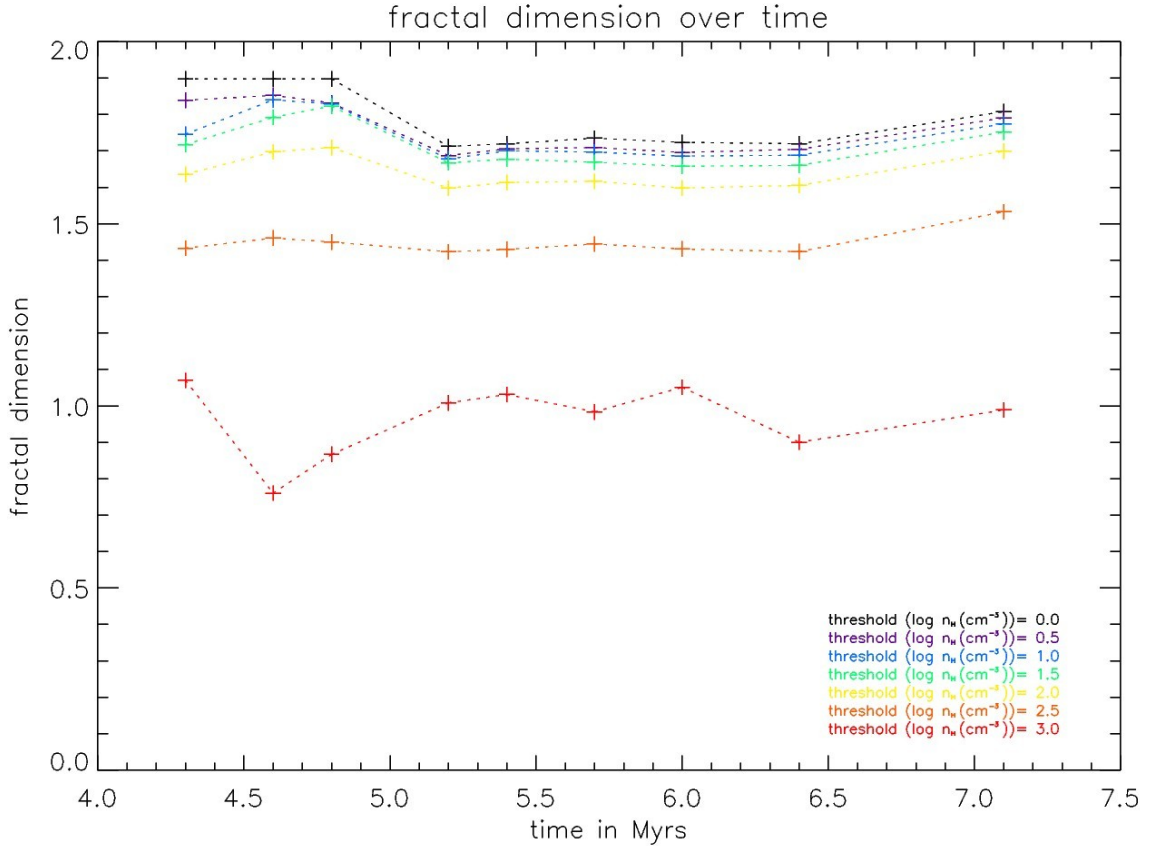


Figure 22: fractal dimension for ongoing time at different thresholds of hydrogen density

Summary

The interstellar medium as it is observed gets its material – especially hydrogen, but also helium – from wind blowing (or exploding) stars of spectral class OB as a reduction of hydrogen in their atmosphere is intended. Those winds that might be momentum driven in the start, but then change to the energy driven type show non-linear behaviour and – combined with turbulences in the shell and cooling instabilities – generate turbulent initial conditions that lead to a fragmentation of the hydrogen superbubbles blown away from the stars. Those turbulences – as well as the extreme scattering events and to a certain degree the influence of self-gravity – play an important role in the process of the formation of interstellar clouds. Note that the hydrogen is not virialized as the gas is not everywhere gravitationally bound.

The fragmentation of colliding superbubbles can be examined by studying the fractal dimension of the hydrogen. Although, different factors can cause problems for estimating the fractal dimension there are methods to calculate its value with quite good results. So though the parameter-area-method as well as the mass-size method – both possibilities to estimate the fractal dimension – are disturbed by effects like noise and opacity the fractal dimension can be calculated using the box-counting method.

The results show that the fractal dimension decreases in a way like

$$D_f \propto -e^{c \cdot th}$$

c being a constant and th being the threshold of hydrogen density. The value of fractal dimension doesn't change by a big amount though the area filled with structure decreases by a non-negligible factor. Finally, the behaviour of the fractal dimension for running time has been shown were it initially increases then drops and finally rises in its value again.

Acknowledgment (engl.)

At this point I would like to thank all the people who made it possible for me to write this Bachelor thesis.

First of all I owe thanks to Prof. Dr. Andreas Burkert who has given the very interesting matter to me. His suggestions and encouragements for the different points of this assignment always cheered me on working with even greater interest on this topic.

I always felt welcome and good being in his work group “Computational Astrophysics” at the University Observatory Munich.

I also want to thank my adviser Evangelia Ntormousi. In addition to providing me the data I used for the plots she always had time and enough patience to answer my questions and helped me in every way one can imagine. It wouldn't have been possible for me to write this assignment without her help.

I would like to thank all my friends who always showed interest in my assignment and let my time at university be a really great and funny one. Without them my university studies wouldn't have worked out as good as they are.

At last big thanks go to my family who always gave me encouragement and who always gave me a good place to return. Cause of them I was able to study physics in the first place. Thanks to their care I always had the strength to go on even in harder times.

Danksagung (dt.)

An dieser Stelle möchte ich allen danken, die es mir ermöglicht haben, diese Bachelor-Arbeit zu verfassen.

Zu aller erst schulde ich Prof. Dr. Andreas Burkert meinen Dank, der mir dieses überaus interessante Thema zugeteilt hat. Seine Vorschläge und Anregungen für verschiedene Punkte, die hier Platz gefunden haben haben mich dazu ermuntert mit noch größerem Interesse an das Thema heranzugehen.

Ich habe mich stets in seiner Arbeitsgruppe „Computational Astrophysics“ an der Universitätssternwarte München wohl gefühlt.

Des weiteren möchte ich meiner Betreuerin Evangelia Ntormousi danken. Sie hat mir nicht nur die Daten, die für die Plots und Auswertungen wichtig waren, gestellt, sondern sie hat mir jederzeit mit genügend Geduld meine Fragen beantwortet und mir in jeder erdenklichen Weise geholfen. Ohne sie wäre es mir nicht möglich gewesen, diese Arbeit zu verfassen.

Ich möchte auch allen meinen Freunden danken, die immer Interesse an meiner Arbeit gezeigt haben und mir eine großartige und fröhliche Zeit an der Universität ermöglichen. Ohne sie wäre mein Studium nicht so gut ausgefallen, wie es der Fall ist.

Zum Schluss möchte ich meiner Familie danken. Sie haben mich zu jeder Zeit unterstützt und in meinem Studium ermuntert und sie gibt mir einen schönen Platz, zu dem ich immer zurückkommen kann. Nur wegen ihr konnte ich überhaupt mit meinem Physikstudium beginnen. Dank ihrer Fürsorge hatte ich immer die Kraft auch in härteren Zeiten, in denen ich nur wenig Zeit für etwas anderes außer dem Studium hatte, weiter nach vorne zu gehen.

Appendix

For the sake of completeness there now will be the figures and plots promised in the previous text and so more. The beginning will be the plots for the hydrogen density on the time steps of 4.3, 4.6, 4.8, 5.2, 5.4, 5.7, 6.0, 6.4 and 7.1 Myr.

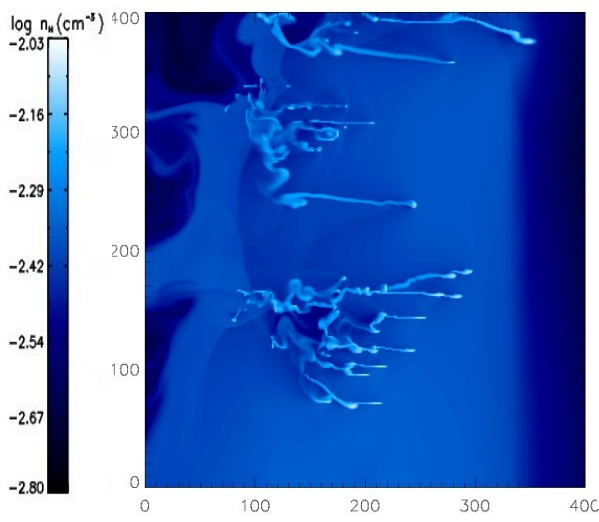


Figure I: density plot for $t = 4.3$ Myr; the axis' units are the number of data points

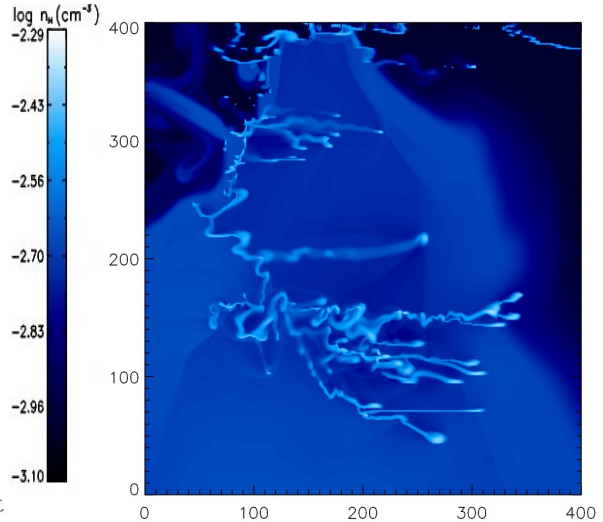


Figure II: density plot for $t = 4.6$ Myr; the axis' units are the number of data points

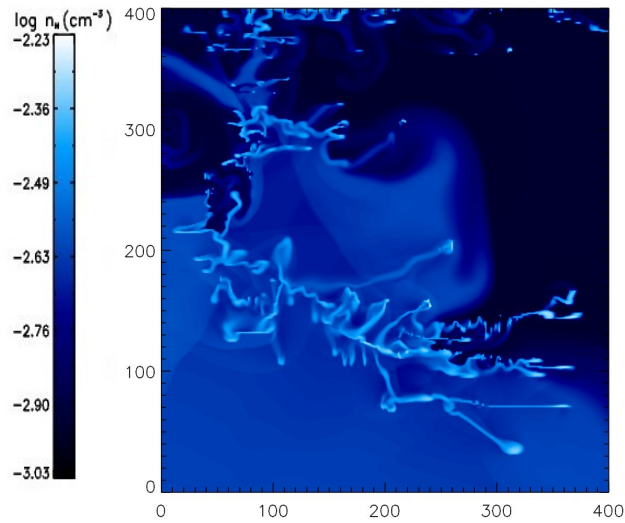


Figure III: density plot for $t = 4.8$ Myr; the axis' units are the number of data points

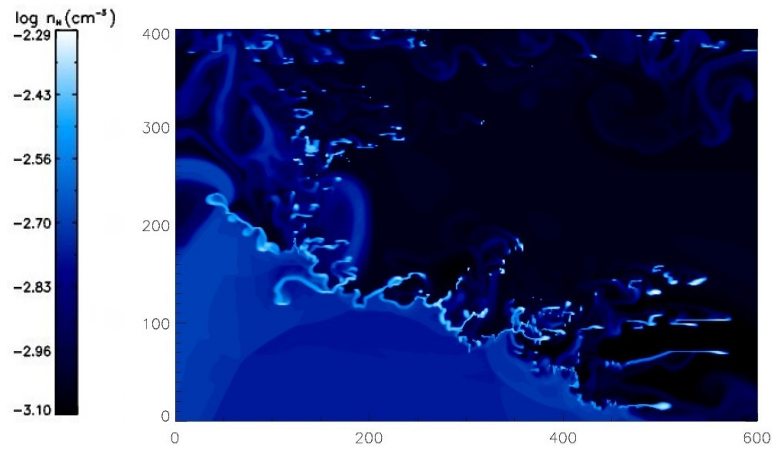


Figure IV: density plot for $t = 5.2$ Myr, the axis' units are the number of data points

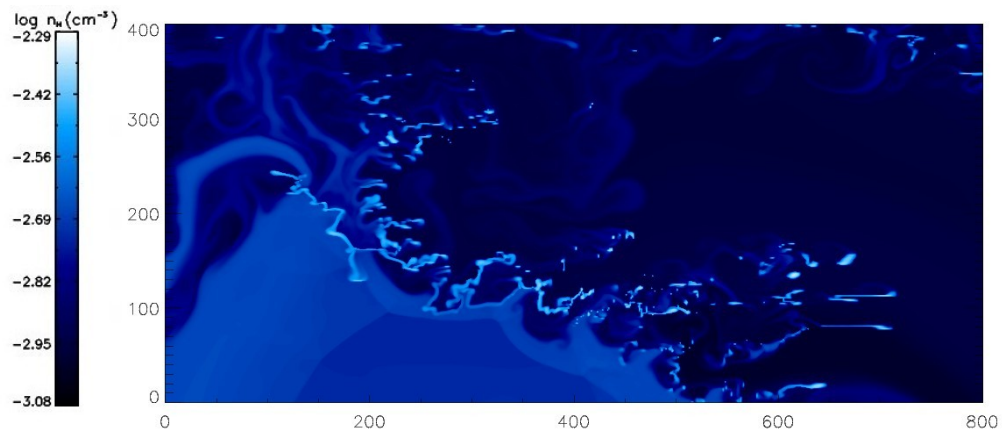


Figure V: density plot for $t = 5.4$ Myr, the axis' units are the number of data points

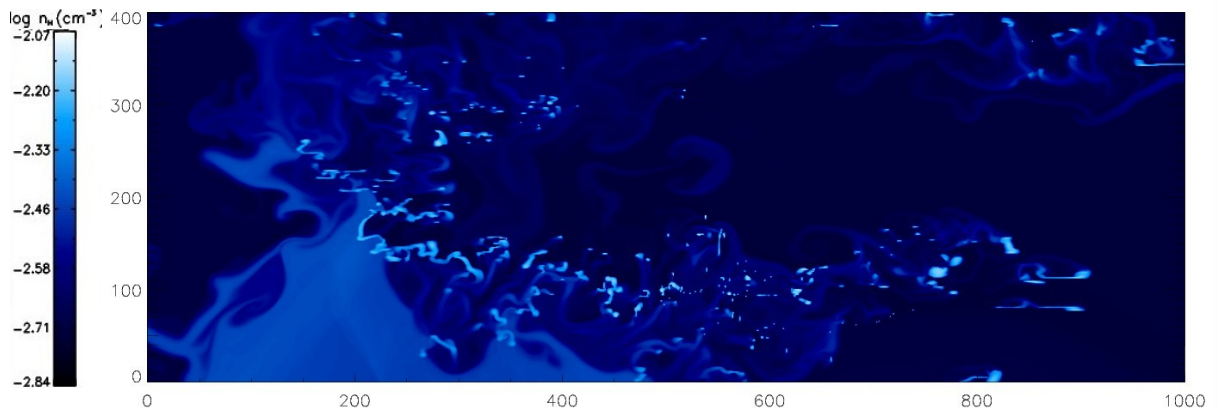


Figure VI: density plot for $t = 5.7$ Myr, the axis' units are the number of data points

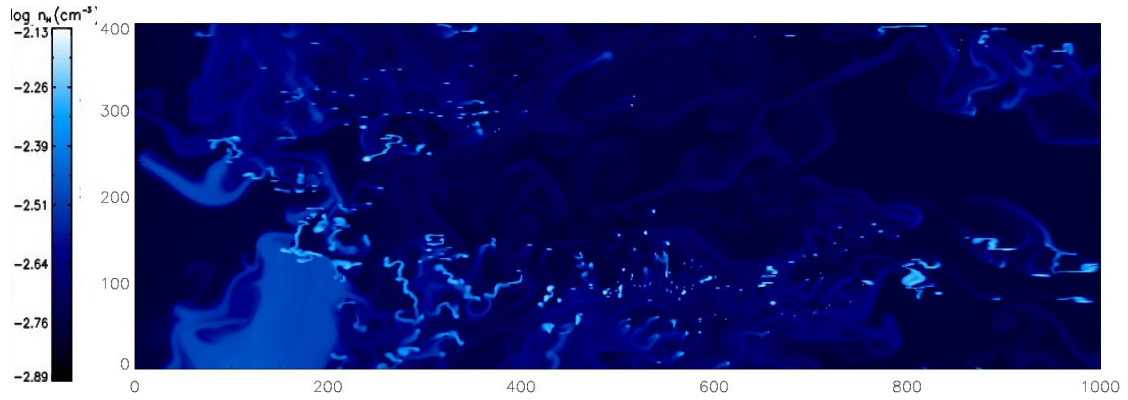


Figure VII: density plot for $t = 6.0$ Myr, the axis' units are the number of data points

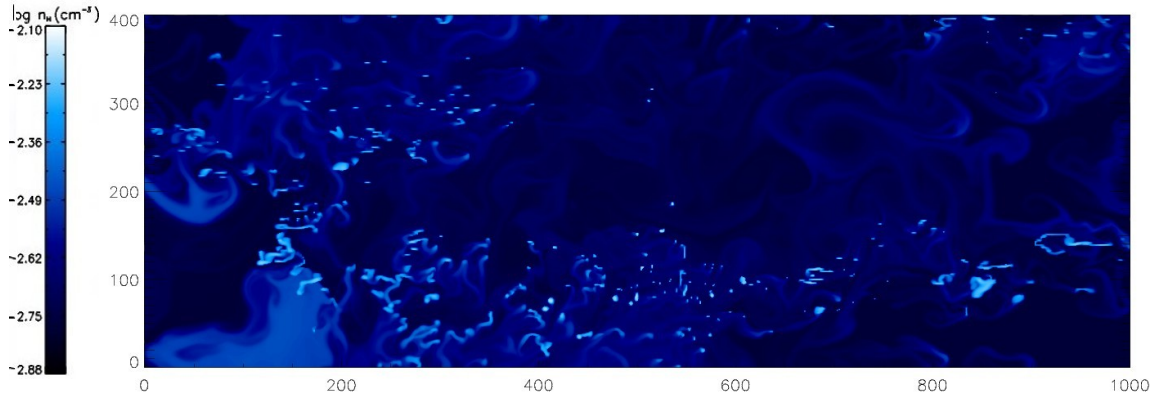


Figure VIII: density plot for $t = 6.4$ Myr, the axis' units are the number of data points

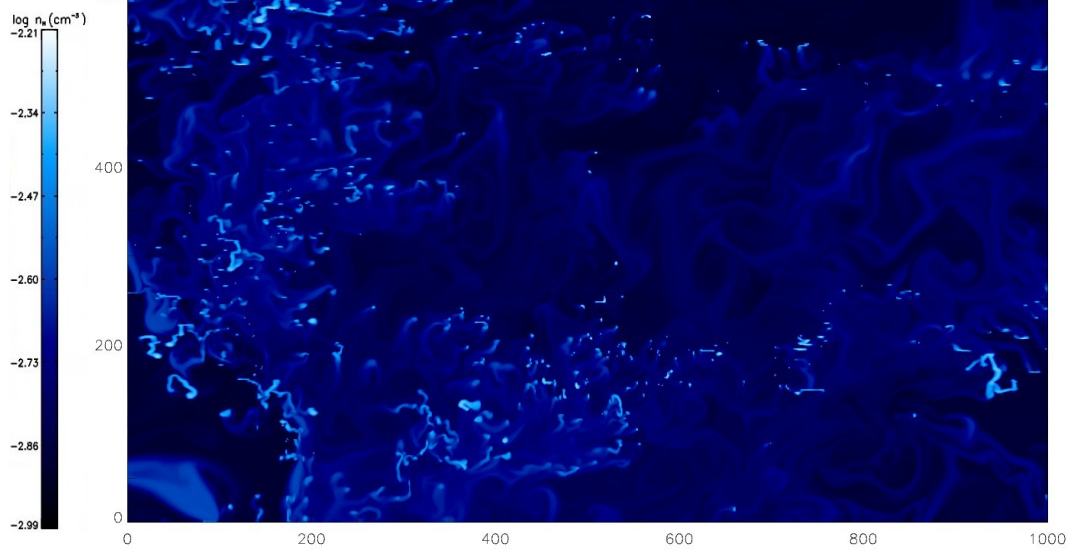


Figure IX: density plot for $t = 7.1$ Myr, the axis' units are the number of data points

Now there will be shown the plots with different density thresholds for different time steps. In addition there will be a threshold- fractal dimension-plot showing a similar behaviour for $t = 4.6, 5.4, 6.0$ and 7.1 Myr.

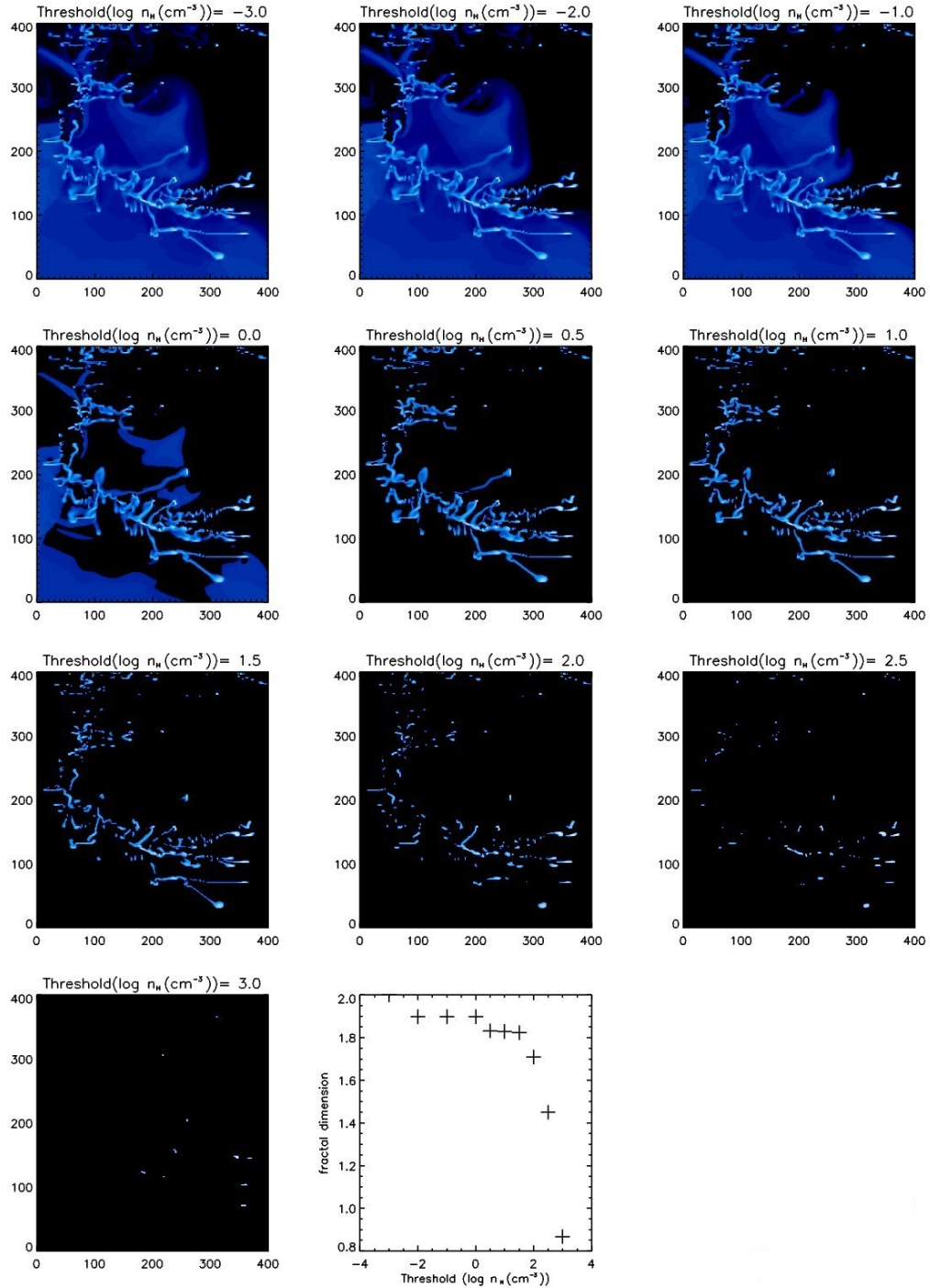


Figure X: density plot for different thresholds at $t = 4.8$ Myr

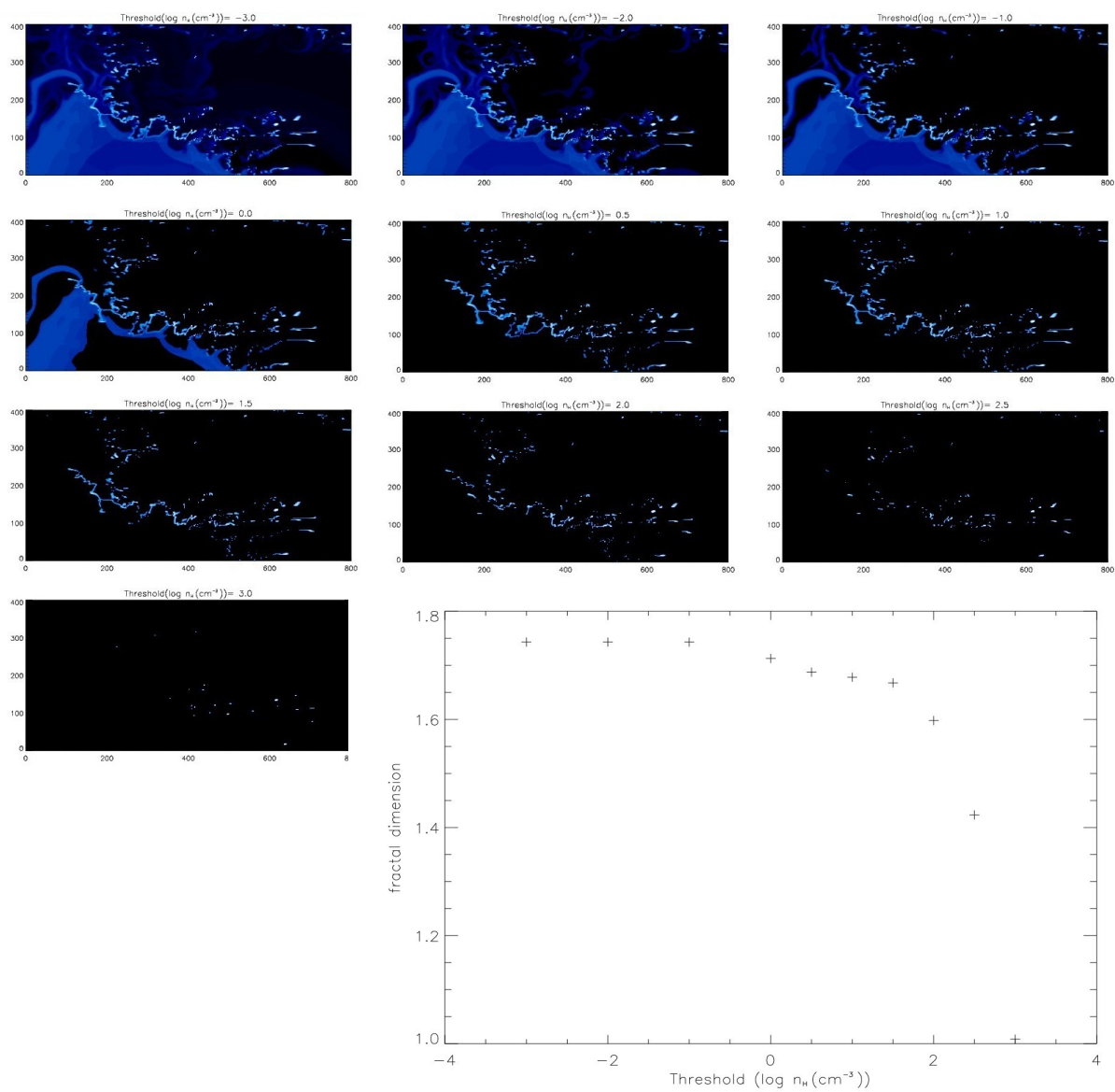


Figure XI: density plot for different thresholds at $t = 5.4$ Myr

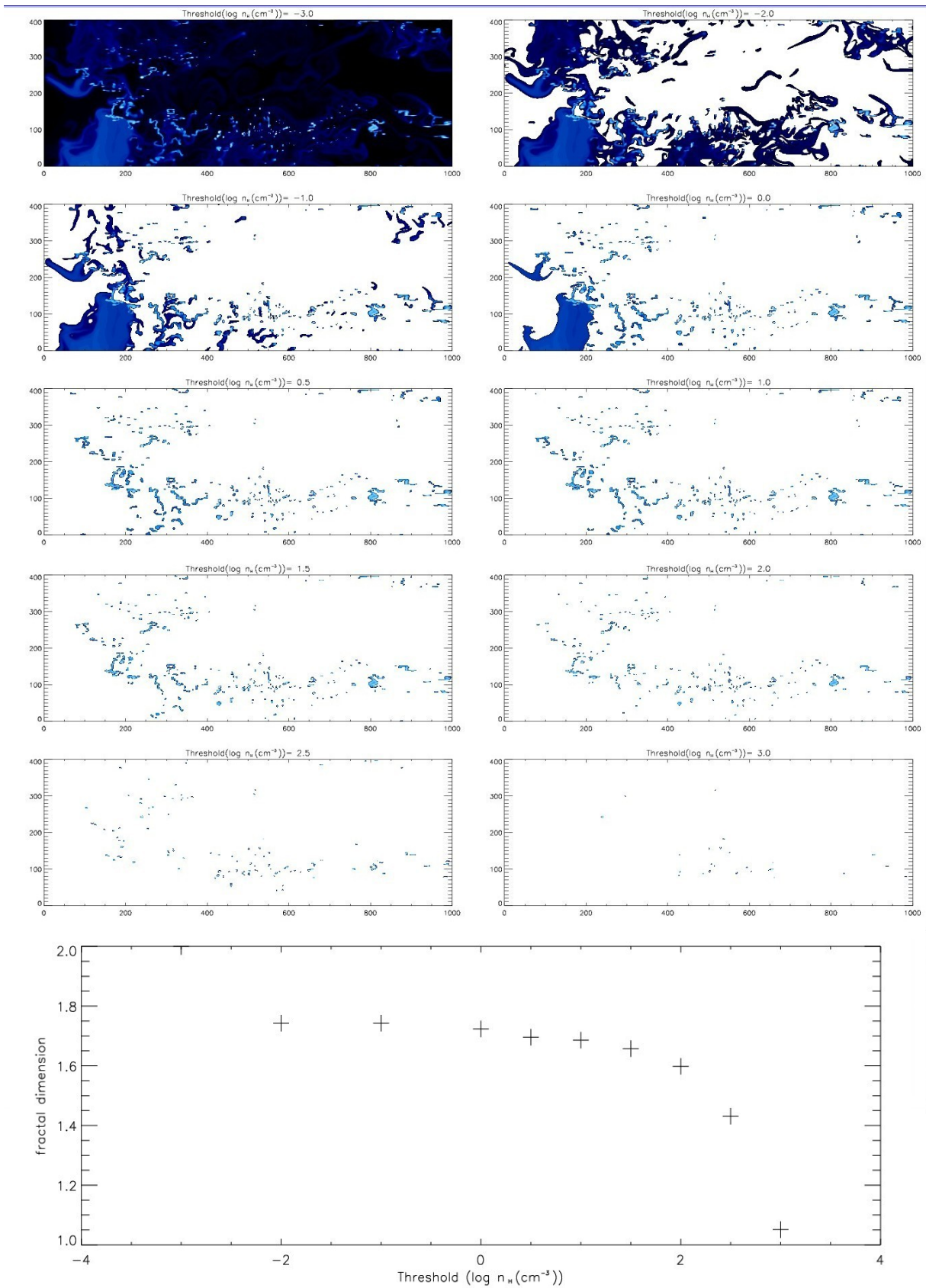


Figure XII: density plot for different thresholds at $t = 6.0$ Myr

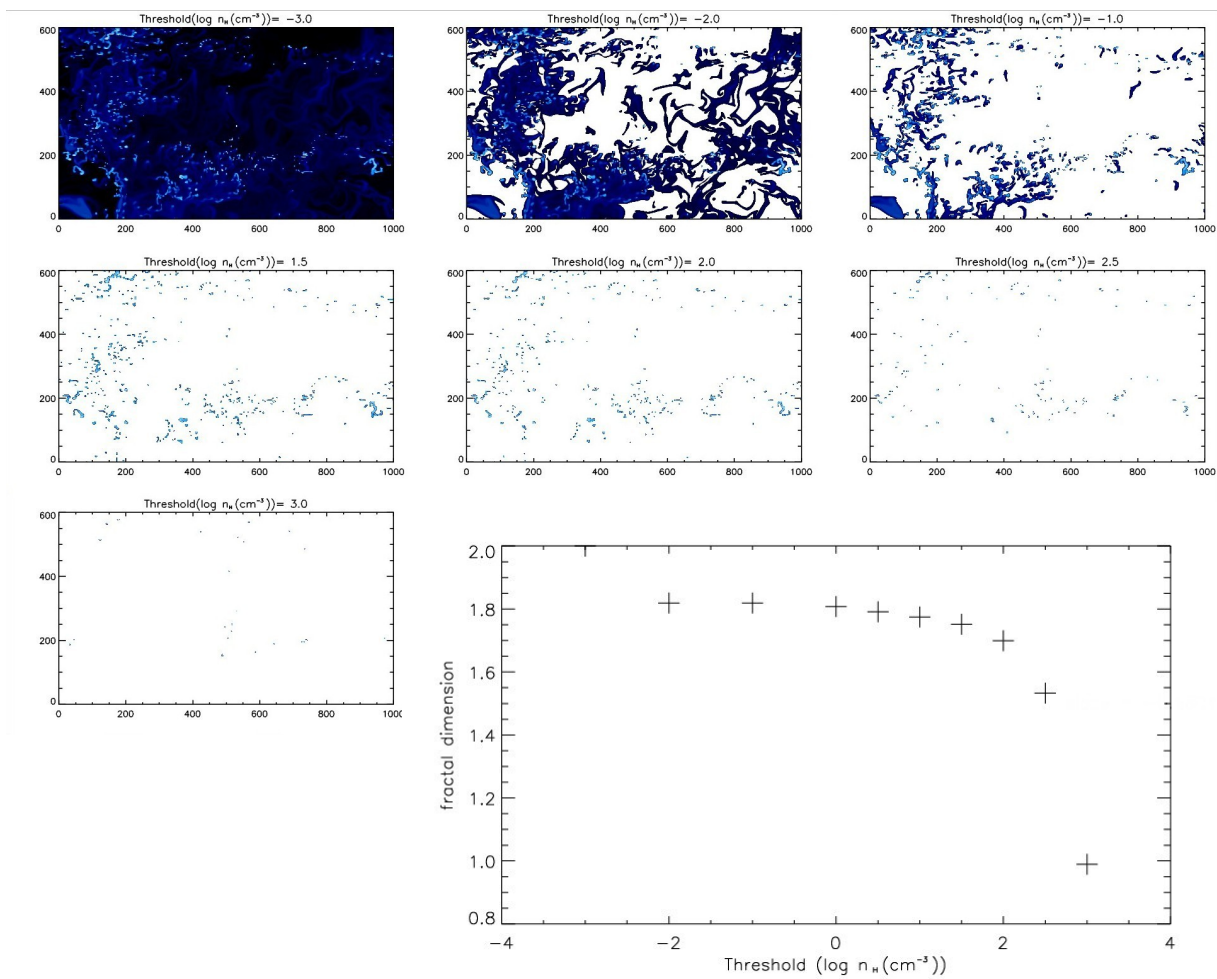


Figure XIII: density plot for different thresholds at $t = 7.1$ Myr

Bibliography

- Burkert, A., Lin, D. N. C., Thermal instability and the formation of clumpy gas clouds. *Astrophysics*, *arXiv:astro-ph/0002106v1*
- Burkert, A. (2006). The turbulent interstellar medium. *Comptes Rendus Physique* 7:433-441
- Combes, F. (1999). Astrophysical fractals: Interstellar medium and galaxies. *Astronomic Astrophysics*: *arXiv: astro-ph/9906477v1*
- Dobbs, C. L., Burkert, A., Pringel, J. E. (2011). Why are most molecular clouds not gravitationally bound? *Monthly Notices of the Royal Astronomical Society, Galaxy Astrophysics*: *arXiv: 1101.3414 [astro-ph.GA]*
- Lazio, T. J. W., Fey, A. L., Gaume, R. A. (2000). Extreme Scattering Events: An Observational Summary. *Astrophysics and Space Science*, 278:155-158
- Mellema, G. and Lundqvist, P. (2002). Stellar wind bubbles around WR and [WR] stars. *Astronomy & Astrophysics*, 394:901-910
- Ntourmoussi, E., Burkert, A., Fierlinger, K., Heitsch, F. (2010). Formation of cold filamentary structure from wind-blown superbubbles. *Astrophysical Journal*, 731:13
- Oey, M. S., Clarke, C. J., Massey, P. (2001). Mechanical Feedback: From Stellar Wind Bubbles to Starbursts. *Astrophysics*, *arXiv: astro-ph/0103302v1*
- Sánchez, N., Alfaro, E. J., Pérez, E. (2005). The fractal dimension of projected clouds. *Astrophysical Journal*, 625:849-856

Sánchez, N., Alfaro, E. J., Pérez, E. (2006). Fractal dimension of interstellar clouds: Opacity and noise effects. *Astrophysical Journal*, 656:222-226

Yadav, J. K., Bagla, J. S., Khandai, N. (2010). Fractal dimension as a measure of the scale of Homogeneity. *Monthly Notices of the Royal Astronomical Society*, 405:2009

http://www.mpipks-dresden.mpg.de/~tisean/TISEAN_2.1/docs/chaospaper/node30.html,
last visit on 11th of Sept.

<http://mathworld.wolfram.com/CorrelationDimension.html>, *last visit on 11th of Sept.*

<http://ese.nrl.navy.mil/>, *last visit on 11th of Sept.*

<http://mathworld.wolfram.com/HeavisideStepFunction.html>, *last visit on 11th of Sept.*

<http://www.thphys.uni-heidelberg.de/~hefft/vk1/k4/424.htm>, *last visit on 11th of Sept.*

<http://www.physik3.gwdg.de/Praktika/Fortgeschrittenen/Versuche/V254/kelvin.pdf>,
last visit on 11th of Sept.

<http://www.bartol.udel.edu/~asif/lors/ntsi.html>, *last visit on 11th of Sept.*

http://www.math.sunysb.edu/~scott/Book331/Fractal_Dimension.html, *last visit on 11th of Sept.*

http://www.nd.edu/~jcaine1/mathematics/limits_chaos.html, *last visit on 11th of Sept.*

<http://classes.yale.edu/fractals/fracanddim/boxdim/KochBoxDim/KochBoxDim.html>,
last visit on 11th of Sept.

<http://math.bu.edu/DYSYS/chaos-game/node6.html>, *last visit on 11th of Sept.*

<http://www.jimloy.com/fractals/koch.htm>, *last visit on 11th of Sept.*

Selbstständigkeitserklärung

Hiermit versichere ich,

dass ich diese Bachelorarbeit zum Thema “Filamentary structure of wind blown superbubbles” selbstständig verfasst habe. Ich habe keine anderen Quellen und Hilfsmittel benutzt, sowie Zitate kenntlich gemacht.

Mir ist bekannt, dass Zuwiderhandlung auch nachträglich zur Aberkennung des Abschlusses führen kann.

Landshut, den 11. September 2011

Ort, Datum

Unterschrift